Effects of Optic Flow in Motor Cortex and Area 7a

H. MERCHANT,[1,2] A. BATTAGLIA-MAYER,[1,2] AND A. P. GEORGOPOULOS[1–5]
[1]*Brain Sciences Center, Department of Veterans Affairs Medical Center, Minneapolis 55417;* [2]*Department of Neuroscience,* [3]*Department of Neurology, and* [4]*Department of Psychiatry, University of Minnesota Medical School; and* [5]*Cognitive Sciences Center, University of Minnesota, Minneapolis, Minnesota 55455*

Received 14 November 2000; accepted in final form 21 May 2001

Merchant, H., A. Battaglia-Mayer, and A. P. Georgopoulos. Effects of optic flow in motor cortex and area 7a. *J Neurophysiol* 86: 1937–1954, 2001. Moving visual stimuli were presented to behaving monkeys who fixated their eyes and did not move their arm. The stimuli consisted of random dots moving coherently in eight different kinds of motion (right, left, up, downward, expansion, contraction, clockwise, and counterclockwise) and were presented in 25 square patches on a liquid crystal display projection screen. Neuronal activity in the arm area of the motor cortex and area 7a was significantly influenced by the visual stimulation, as assessed using an ANOVA. The percentage of cells with a statistically significant effect of visual stimulation was 3 times greater in area 7a (370/587, 63%) than in motor cortex (148/693, 21.4%). With respect to stimulus properties, its location and kind of motion had differential effects on cell activity in the two areas. Specifically, the percentage of cells with a significant stimulus location effect was ~2.5 times higher in area 7a (311/370, 84%) than in motor cortex (48/148, 32.4%), whereas the percentage of cells with a significant stimulus motion effect was ~2 times higher in the motor cortex (79/148, 53.4%) than in area 7a (102/370, 27.6%). We also assessed the selectivity of responses to particular stimulus motions using a Poisson train analysis and determined the percentage of cells that showed activation in only one stimulus condition. This percentage was 2 times higher in the motor cortex (73.7%) than in area 7a (37.7%). Of all kinds of stimulus motion tested, responses to expanding optic flow were the strongest in both cortical areas. Finally, we compared the activation of motor cortical cells during visual stimulation to that observed during force exertion in a center → out task. Of 514 cells analyzed for both the motor and visual tasks, 388 (75.5%) showed a significant relation to either or both tasks, as follows: 284/388 (73.2%) cells showed a significant relation only to the motor task, 27/388 (7%) cells showed a significant relation only to the visual task, whereas the remaining 77/388 (19.8%) cells showed significant relations to both tasks. Therefore a total of 361/514 (70.2%) cells were related to the motor task and 104/514 (20.2%) were related to the visual task. Finally, with respect to receptive fields (RFs), there was no clear visual receptive field structure in the motor cortical neuronal responses, in contrast to area 7a where RFs were present and could be modulated by the type of optic flow stimulus.

INTRODUCTION

It is an essential aspect of our interaction with the environment that we deal with objects in it (i.e., reach, catch, etc.). Many times the subject and the object are immobile but frequently the subject (i.e., during forward locomotion), the object (i.e., a mosquito), or both (e.g., a catcher and a falling ball) are in relative motion with respect to each other. Such cases are frequent and meaningful in the motor repertoire of an animal. This is especially true for primates, given the exquisite development of their visual system, which enables them to detect, analyze, and interact effectively with objects around them. An additional advantage of the primates is the excellent use they possess of the arm for reaching and of the hand for grasping. It is not surprising that the conjunction of outstanding visual and motor capacities confers to primates such an exceptional status in visuomotor coordination. Now, a wealth of evidence obtained during the last 30 years of research indicates that area 7a of the posterior parietal lobe and the motor cortex play a central node in visuomotor coordination. On the one hand, area 7a is engaged in a wide variety of sensorimotor processes and responses to visual moving stimuli, including optic flow (Andersen 1997; Motter and Mountcastle 1981; Mountcastle et al. 1975; Siegel and Read 1997). On the other hand, motor cortex is involved in several aspects of movement initiation and control, including the motor command itself as well as processes interposed between a stimulus and the response to it (Alexander and Crutcher 1990a,b; Evarts 1981; Georgopoulos et al. 1982, 1986, 1989, 1992; Zhang et al. 1997). In addition, responses of motor cortical neurons to simple moving stimuli have been described (Port et al. 2001; Wannier et al. 1989). However, no detailed investigation of motor cortical responses to optic flow stimuli have been performed. It would be of interest to know whether such responses exist, and if so, to compare the functional properties of motor cortex and area 7a during optic flow stimulation. This information can provide important insights about the processing of visual motion used in action. In the present study, we investigated the responsiveness of cells in the motor cortex and area 7a to optic flow visual stimuli. The results showed the following: *1*) in both cortical areas there are preferential responses to expanding optic flow; *2*) the large majority of neurons responded selectively to one type of optic flow stimuli, particularly in the motor cortex; *3*) the receptive field (RF) structure in area 7a neurons could be modulated by the type of optic flow stimulus; *4*) there was no clear visual RF structure in the motor cortical neuronal responses, and therefore the modulation of motor cortical cell activity by optic flow stimuli did not depend on a RF structure; and *5*) the magnitude of the effects of visual stimulation observed, although smaller, was comparable to those observed

Address for reprint requests: A. P. Georgopoulos, Brain Sciences Center (11B), VAMC, One Veterans Dr., Minneapolis, MN 55417 (E-mail: omega @umn.edu).

The costs of publication of this article were defrayed in part by the payment of page charges. The article must therefore be hereby marked "*advertisement*" in accordance with 18 U.S.C. Section 1734 solely to indicate this fact.

Downloaded from www.physiology.org/journal/jn at Univ of Minnesota (134.084.001.059) on April 13, 2019.

in the same motor cortical cells during force exertion on a manipulandum.

METHODS

Animals

Two male monkeys (*Macaca mulatta*, 6 and 7 kg body wt) were used in this study. Animal care conformed to the principles outlined in the *Guide for Care and Use of Laboratory Animals* (National Institutes for Health publication no. 85-23, revised 1985). Animal studies protocols were approved by the local institutional review boards.

Visual stimuli

Stimuli were presented on a 69 cm × 69 cm tangent screen placed 48.5 cm in front of the animal. Small square patches of random dots were presented successively at 25 different positions in a regular 5 × 5 grid (Fig. 1*A*). The dots could move in eight different motion conditions (Fig. 1*B*): the four cardinal directions of translation (rightward, leftward, upward, and downward), expansion, contraction, clockwise (CW) rotation, and counterclockwise (CCW) rotation. Stimuli were back-projected on the screen using a liquid crystal display projector (NEC Multisync MT 820/1020) with a refresh rate of 60 Hz. The whole screen subtended 71° of visual angle (DVA), at eye level. The small square patches were 13.8 cm × 13.8 cm and subtended 16.2 DVA on a side at the center of the screen; the DVA subtended was progressively smaller away from the center of screen. Stimuli were presented within such a patch for 400 ms, one patch at a time, with an inter-patch presentation interval of 150 ms. The stimuli were composed of 30 white dots moving within a square on a black background. Each dot was a circle of 0.35 DVA in diameter and moved for a maximum lifetime of 400 ms, after which it was assigned to a new random location within a square patch. If a moving dot traveled outside the patch displayed, it was relocated to a new random location within the square. The dots were relocated asynchronously, to avoid coherent flickering of the stimuli. This constant reshuffling essentially eliminated pattern and density artifacts, because the pattern of dots was changing constantly and each region within the square had approximately the same number of points at any time. The linear (constant) velocity in the four directions of translation (left-, right-, up-, and downward), and the directions of expansion and contraction was 40 DVA/s; the angular speed in both directions of rotation was 430°/s. These speeds were in the range of values used in studies by

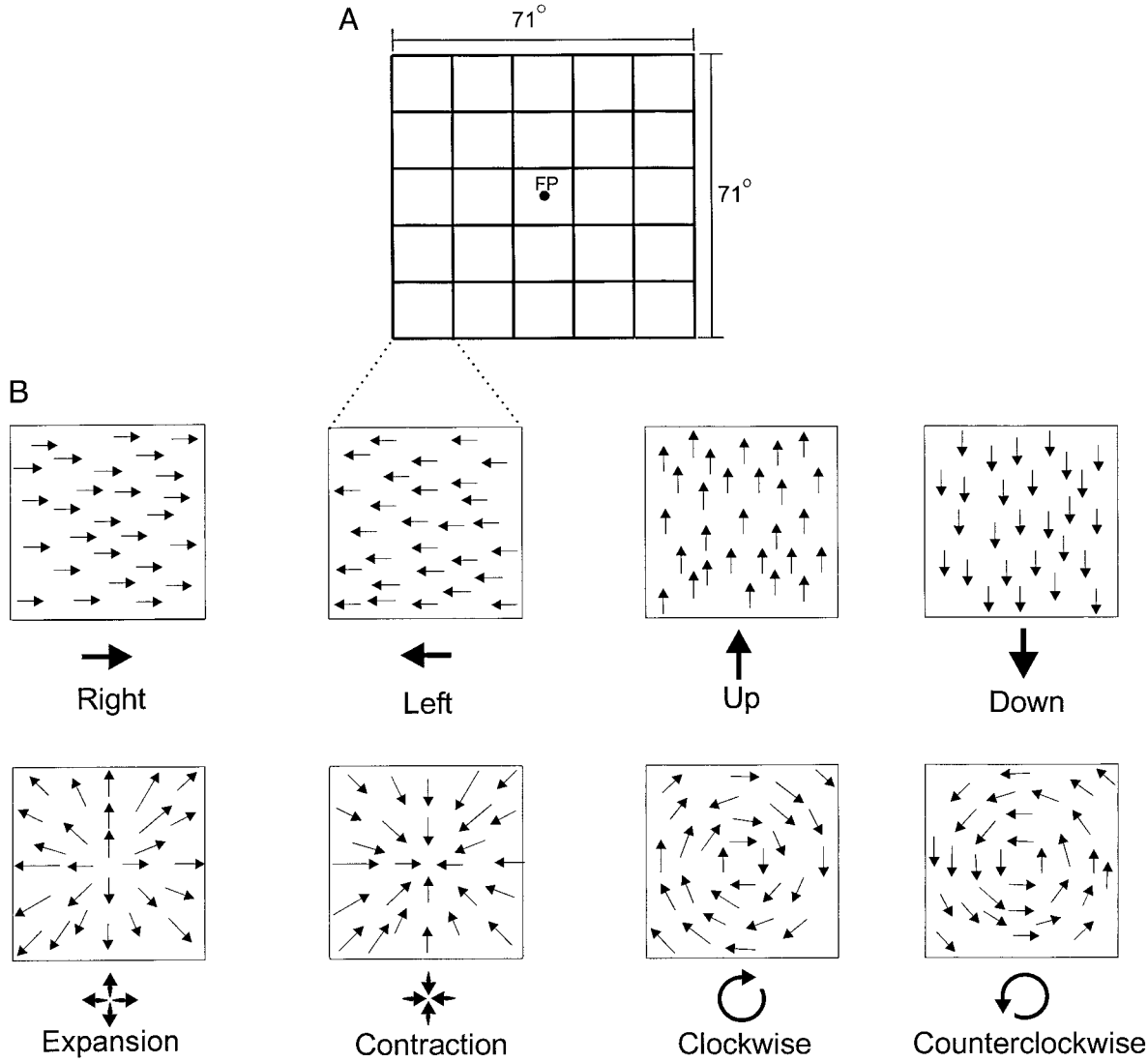

FIG. 1. *A*: 5 × 5 grid of the 25 square patches where stimuli were presented. *B*: 8 kinds of optic flow stimuli used. FP, fixation point.

Downloaded from www.physiology.org/journal/jn at Univ of Minnesota (134.084.001.059) on April 13, 2019.

other investigators (see, e.g., Graziano et al. 1994; Lagae et al. 1994). Since the main objective of this study was to evaluate the effect on neuronal activity of the different kinds of stimulus motion, the location of stimulation and their interaction, no special attempt was made to define a velocity sensitivity curve.

Statistical design

The eight different motion conditions were interleaved and presented in a pseudorandom order. The 25 different patch locations were nested within each stimulus motion condition and were also presented pseudorandomly. A complete run consisted of the presentation of all conditions in three repetitions. We wanted to assess the statistical significance of the effect on cell activity of two factors, namely stimulus motion condition (at $k = 8$ levels) and stimulus location (at $m = 25$ levels). The experimental design above was a nested, complete factorial design in which all eight stimulus motion conditions were tested for each 1 of the 25 stimulus locations. These presentations were blocked in three repetitions. This number of repetitions was chosen based on statistical considerations, namely that adequate degrees of freedom (DF) for the error terms would be available to assess the effects of stimulus motion condition, stimulus location, and their interaction. Specifically, there were eight stimulus motion conditions $\times$ 25 stimulus locations $\times$ 3 repetitions = 600 trials, yielding a total of $DF_{total} = 599$; the DF for the error term were $DF_{error} = DF_{total} - DF_{motion} - DF_{location} - DF_{repetition} = 599 - 7 - 24 - 2 = 566$; the DF of the F statistic for testing the stimulus Motion effect were [7,566] and for testing the stimulus Location effect [24,566]. These are more than adequate error DF for the tests planned, and further increase in them (by increasing the number of repetitions) would not have improved the sensitivity of the F statistic used to assess the stimulus Motion and Location effects. For example, suppose that the number of repetitions was increased to a large number such that the error DF were now 10,000. In this case, the values of the F statistic (at $\alpha = 0.05$) for [7,566] and [7,10000] degrees of freedom are $\sim$2.0263 and 2.0105, which is a rather trivial reduction in the F value (i.e., increase in the sensitivity of the test), as compared with the huge increase of the error degrees of freedom (stemming from the increased number of repetitions) from 566 to 10,000. Similarly, the corresponding values for the F testing the effect of stimulus location for [24,566] and [24,10000] degrees of freedom are and 2.0105 are $\sim$1.5373 and 1.5184, which again are trivially close to justify the increase in repetitions. Therefore three repetitions were adequate for the purposes of this study.

Tasks

The monkeys (*monkeys 1* and *2*) were seated in a primate chair with the left arm loosely restrained. In the visual stimulation task, a yellow spot of 0.32 DVA diameter served as the fixation point (FP) and was presented in the center of the translucent tangent screen. The monkeys were trained to fixate this spot (within 2 DVA) for the duration of stimulus presentation. During that time, *monkey 1* maintained the right hand in a relaxed position (monitored using a video camera), whereas *monkey 2* maintained grasp of a vertical semi-isometric joystick with the right hand by exerting a constant pulling force on the joystick of $\sim$0.22 N. First, the FP was turned on which the monkeys fixated; following attainment of fixation, 100–500 ms were allowed for *monkey 2* to grasp the joystick. Then, stimuli were presented on the screen. A juice reward was delivered randomly every 1.1–3.3 s while fixation was maintained; if fixation was broken, the trial was aborted. The *X*-*Y* eye position was monitored using an oculometer (Dr. Bouis, Karlsruhe, Germany). Both the eye and the joystick position were sampled at 200 Hz; the tangential eye velocity was calculated by differentiating eye position.

In the center $\rightarrow$ out motor task, the monkeys produced semi-isometric force pulses on the joystick in eight radial directions, in response to the presentation of a peripheral target on an imaginary circle of 0.89 N radius. A force feedback cursor on the screen indicated the current net force exerted on the joystick; a constant upward bias of 0.108 N was applied, corresponding to a deflection of the cursor of 0.85 DVA. A trial began with the appearance of a light spot at the center of the screen that prompted the monkey to exert a downward force of 0.108 N on the joystick to align the force feedback cursor to the center spot within a circular force window of 0.217 N radius. Then, after a variable delay of 1–3 s, a light spot appeared on an imaginary circle of 6.8 DVA, which prompted the monkey to apply a force pulse ($>$0.89 N) on the joystick such that the force feedback cursor would move in the direction of the peripheral stimulus for the monkey to obtain a liquid reward. Five repetitions of this task were performed in a randomized block design.

Neural recordings

At the end of the training period, two stainless steel recording chambers were implanted, one in the arm representation of the motor cortex and the other in area 7a of the posterior parietal cortex. In addition, four titanium posts were positioned on the scull to support a halo used to immobilize the head during the experiment. These procedures were conducted under aseptic conditions and general anesthesia.

The electrical activity of single neurons in the motor cortex and area 7a was recorded extracellularly using a system with seven independently movable microelectrodes (Uwe Thomas Recording, Marburg, Germany) (see Lee et al. 1998; Mountcastle et al. 1991). The electrodes were flexible quartz coated platinum-tungsten alloy fibers with 1–3 MΩ of impedance at 1,000 Hz. All the isolated neurons were recorded regardless of their activity during the task and the recording sites changed from session to session.

Each electrode signal was amplified, filtered, and monitored using display oscilloscopes (Tektronix 2232). The action potentials were isolated using a dual-amplitude window discriminator (Bak Electronics, Germantown, MD) and multispike discriminators (MSD, Alpha-Omega Engineering, Nazareth, Israel). The presentation of the visual stimuli, behavioral control, and data collection was carried out by a personal computer. On-line raster displays were generated on a computer monitor. Finally, the depth from the top of neural activity at which each cell was recorded was noted and retained in a separate record.

The recording area was identified by marking the center of the recording chamber with a stainless steel pin placed directly in the brain, just before the monkey was killed with an overdose of pentobarbital sodium. Due to the large number of penetrations, no histological reconstruction of the recording sites was attempted. However, the entry points of the penetrations were plotted on the cortical surface, based on the entry points of the pins above demarcating the recording area. This, together with the recording depth, provided adequate information on the cortical areas sampled.

Electromyographic (EMG) activity

The EMG was recorded in the same two monkeys in separate sessions from the neural recordings using intramuscular, multistranded, teflon-coated wire electrodes (Schwartz et al. 1988). EMG activity of the following muscles was recorded in the first monkey, contralateral to the recording side: rhomboideus major, trapezius, deltoideus (anterior, middle, and posterior), pectoralis major, triceps brachii, biceps brachii, extensor digitorum communis, and forearm flexor (unspecified). The same muscles were recorded from in the second monkey, with the addition of supraspinatus, infraspinatus, and latissimus dorsi. The EMG signal was amplified, rectified, filtered, and sampled at 200 Hz. To assess the variability of the EMG signal, we computed the coefficient of variation (CV) of the average EMG

Downloaded from www.physiology.org/journal/jn at Univ of Minnesota (134.084.001.059) on April 13, 2019.

recorded during the last 300 ms of the 400-ms-long visual stimulation at each of the 25 patch locations for each stimulus motion condition

$$\text{CV} = (\text{standard deviation/mean}) \times 100$$

This gave 200 values (25 locations × 8 stimulus motion conditions) of CV per muscle. Since the CV is a ratio, data were log-transformed and the mean calculated for each muscle. Finally, a grand mean was computed across all 23 muscles studied, and the antilog of that value (i.e., the geometric mean) was calculated.

General data analysis

An initial three-factor ANOVA (Repetition, stimulus Location and stimulus Motion condition) was performed for each neuron to identify cells whose activity changed significantly during repeated stimulus presentations (i.e., cells with a statistically significant effect of Repetition); this was taken to indicate an instability of cell's responsiveness to the stimuli, and, therefore these cells were excluded from further analyses. The frequency of discharge (based on spike counts) during the last 300 ms of the 400-ms-long visual stimulation period was the dependent variable. The spike counts were square-root transformed to stabilize the variance (Cox and Lewis 1966; Snedecor and Cochran 1989; Tukey 1977). A total 1,110 cells were recorded in motor cortex (593 in *monkey 1* and 517 in *monkey 2*) and 959 in area 7a (526 in *monkey 1* and 433 in *monkey 2*). Of these, 693 cells in motor cortex and 587 in area 7a did not show a statistically significant effect of Repetition and were analyzed further. A second, repeated measures ANOVA was then used to assess the statistical significance of the Motion condition and Location effects. The results of this ANOVA were consistent between monkeys in both cortical areas and were combined.

A similar analysis was performed on the motor cortical cell activity during the center → out task, as follows. The square-rooted frequency of discharge (based on spike counts) during the time period from the onset of the peripheral stimulus until the delivery of reward (total experimental time, TET) was computed, and an ANOVA was performed to identify cells whose activity changed over time, using Repetition and Direction as factors. Of a total 941 motor cortical cells recorded during this task (447 in *monkey 1* and 494 in *monkey 2*), 761 did not show a statistically significant effect of Repetition and were analyzed further by performing a second, repeated measures ANOVA to assess the statistical significance of Direction on cell activity as well as the change in activity during TET from that observed during the control period (CP; 500 ms preceding the onset of the peripheral stimulus), defined as a TET-CP contrast. Cells that showed any significant effect of the factors tested (i.e., Direction, Change from the control period, or their Interaction) were deemed to be significantly related to the motor task. The results of this ANOVA were consistent between monkeys and were combined. The program 2V of the BMDP/Dynamic statistical package (BMDP Statistical Sotfware, Los Angeles 1992) was used to execute the ANOVA. The level of statistical significance to reject the null hypothesis for all statistical analyses was set at $\alpha = 0.05$.

Analyses of response magnitude during visual stimulation

The following measures of the magnitude of cell response were calculated for those cells that showed a significant stimulus motion condition effect in the motor cortex and area 7a. *1*) The discharge frequency of a cell was averaged across the 25 stimulus locations and the 3 repetitions, thus yielding 8 values, 1 for each stimulus motion condition. These values were ranked, with *rank 1* denoting the highest activity. Then, the percentage of times for which each condition was ranked *1* was calculated. This provided a nonparametric, robust measure of preference of a particular stimulus motion in the population. *2*) A measure of preference based on both the rank and discharge rate was computed by multiplying the number of times for which a particular stimulus motion condition was *1* times the average frequency of discharge during that condition.

Comparison of motor cortical response magnitude in the visual and motor tasks

Three measures were calculated to compare the magnitude of response between the visual and motor tasks: *1*) the average discharge rate during the control period of the motor task; *2*) the maximum of eight average discharge rates (1 per force direction), from the onset of the peripheral stimulus to the time that the force exerted exceeded the threshold in the motor task; and *3*) the maximum average rate among the eight stimulus motion conditions. To account for possible variation of response due to the location of the stimulus, the maximum response in a given condition was calculated 1st, from among the 25 locations. This last measure was also computed for area 7a cell during the visual task. A paired *t*-test was used to assess the statistical significance of the differences tested.

Finally, the data analyzed came from tasks that comprised directional variables; therefore several directional analyses were carried out, as follows. *1*) In the motor center → out task, the presence of directional tuning was assessed using bootstrap (Lurito et al. 1991) and, if present, the preferred direction was calculated. *2*) In the visual task, there were two distinct cases. First, the direction of the center of the stimulated patch was calculated using the center of the display as the origin of the unit circle. Since the aim of this analysis was to compare directional responses in the center → out task to directional responses in other tasks, the length of the vector from the center of the display to the center of a patch was ignored, and only the direction of the vector was retained. Then the directional tuning and preferred direction were assessed as described above. Finally, the second case in the visual task concerns the stimulus motion condition itself. Specifically, directional tuning and preferred direction was assessed using the left-, right-, up-, and downward directions of stimulus motion (across all patches) as the directional variable.

Effect of transformation

The statistical analyses above were performed on square-rooted discharge rates. Although this is an appropriate transformation (Cox and Lewis 1966; Snedecor and Cochran 1989; Tukey 1977), we also analyzed the data without any transformation with very similar results (see *Neural responses to optic flow stimuli*).

Poisson train analysis

The specificity of a cell response to a particular stimulus condition was assessed using the Poisson train analysis (Hanes et al. 1995). This analysis determines how improbable it is that the number of spikes within a specific time interval is a chance occurrence. For this purpose, the actual number of spikes within a time interval is compared with the number of spikes predicted by the Poisson distribution derived from the mean discharge rate during the entire time period (400 ms in this case). The measure of improbability is the surprise index (SI) defined as

$$\text{SI} = -\ln P$$

where P is defined by the Poisson formula

$$P = e^{-rT} \sum_{i=n}^{\infty} \frac{(rT)^i}{i!}$$

In this equation, P is the probability that, given the average spike train r, a spike train of a time interval T contains n or more spikes. Thus a large SI indicates a low probability that a specific elevation in activity was a chance occurrence.

Downloaded from www.physiology.org/journal/jn at Univ of Minnesota (134.084.001.059) on April 13, 2019.

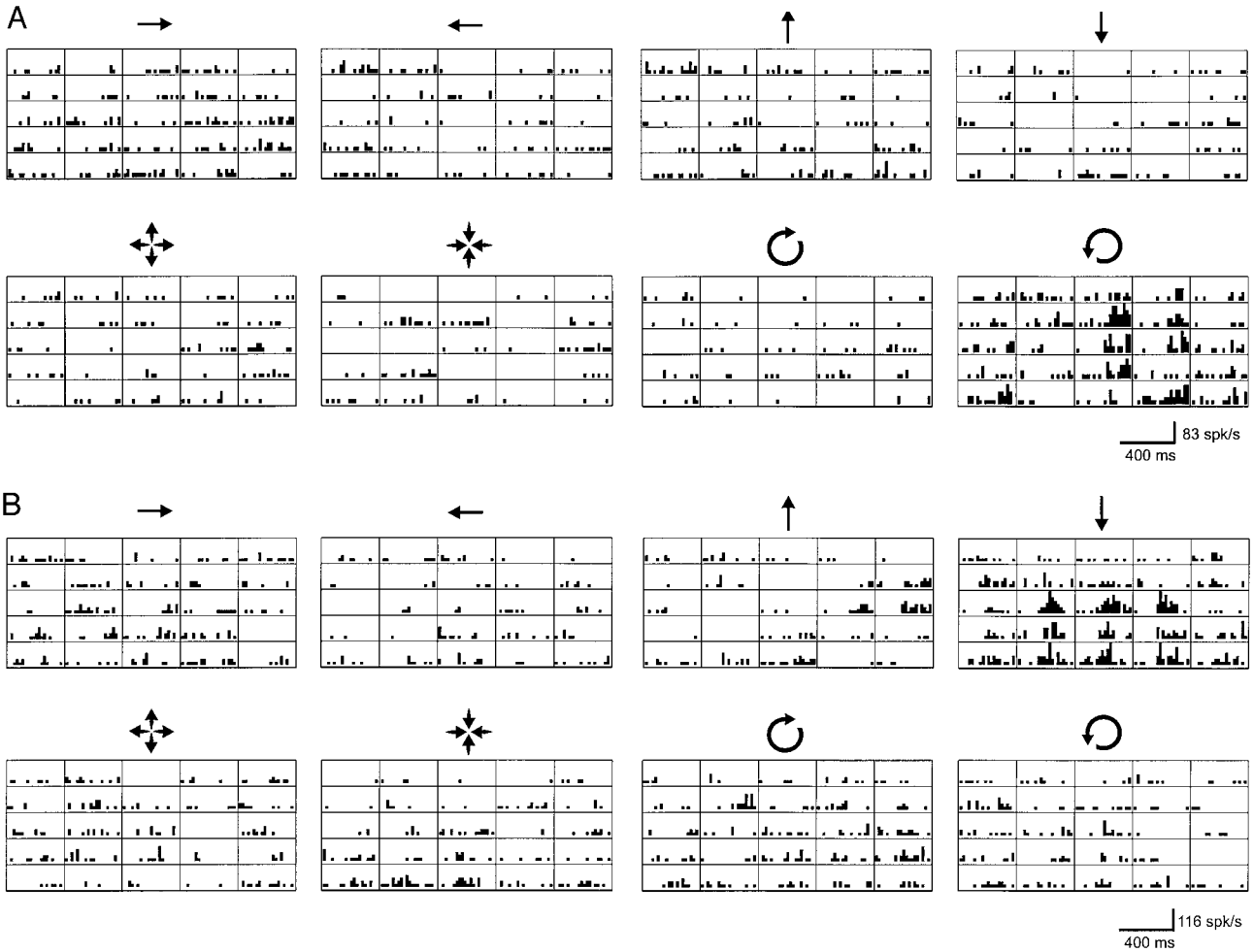

FIG. 2. Responses of a motor cortical (*A*) and an area 7a (*B*) cell to the stimuli used. Peristimulus time histograms (20-ms binwidth) are shown for each Location and stimulus Motion condition.

The spike train analysis was applied for each motion condition, collapsing the times of occurrence of action potentials across repetitions ($n = 3$) and stimulus Locations ($n = 25$). We used the algorithm of Hanes et al. (1995) to detect an activation above randomness, as follows. The mean discharge rate (r) was computed for the 400 ms of stimulus presentation. The first two consecutive spikes that had a mean discharge rate greater or equal to r was found, and the time between these two spikes was defined as the initial T value. Then, the next spike was identified and the interspike interval between this and the previous spike was added to T. The corresponding SI was calculated. This was repeated until the end of the spike train; the spike at the end of the interval T with the maximum SI was defined as the end of the burst. Next, the SI was calculated for the interval T from the last to the first spike. Then, the spikes from the beginning were removed until the end of the spike train, computing the corresponding SI in each step. The spike at which SI was maximized was defined as the beginning of the burst. If the SI from the beginning to the end of the burst was >5.3 (corresponding to $P = 0.005$), then the particular Motion condition was deemed to have a significant effect on cell activity. If this criterion was not fulfilled, it was assumed that there was no response to the stimulus for that case. We found few cases with more than one significant burst, and in this situation we choose the longest burst as the period of activation.

TABLE 1. *Numbers and percentages of neurons with the noted effects in the ANOVA*

Effect	Motor Cortex	Area 7a
Motion condition only	68 (45.9)	35 (9.4)
Stimulus Location only	40 (27)	220 (59.5)
Motion × Location Interaction only	27 (18.2)	20 (5.4)
Motion and Location	6 (4)	41 (11)
Motion and Interaction	5 (3.4)	4 (1.1)
Location and Interaction	2 (1.3)	28 (7.5)
Motion and Location and Interaction	0 (0)	22 (5.9)
Total	148 (100)	370 (100)

Numbers in parentheses are percentages.

Response latency analysis

The onset time of increase in activity for the cells analyzed was determined from the results of the Poisson train analysis above. Specifically, the onset time of a significant increase in cell of activity was taken to be the beginning of the burst or activation. Similarly, the offset times were determined and the duration of the response calculated. These different measures were compared between areas and among stimulus motion conditions.

Visual RF analysis

The following double Gaussian function (Barlow 1989) was used

Downloaded from www.physiology.org/journal/jn at Univ of Minnesota (134.084.001.059) on April 13, 2019.

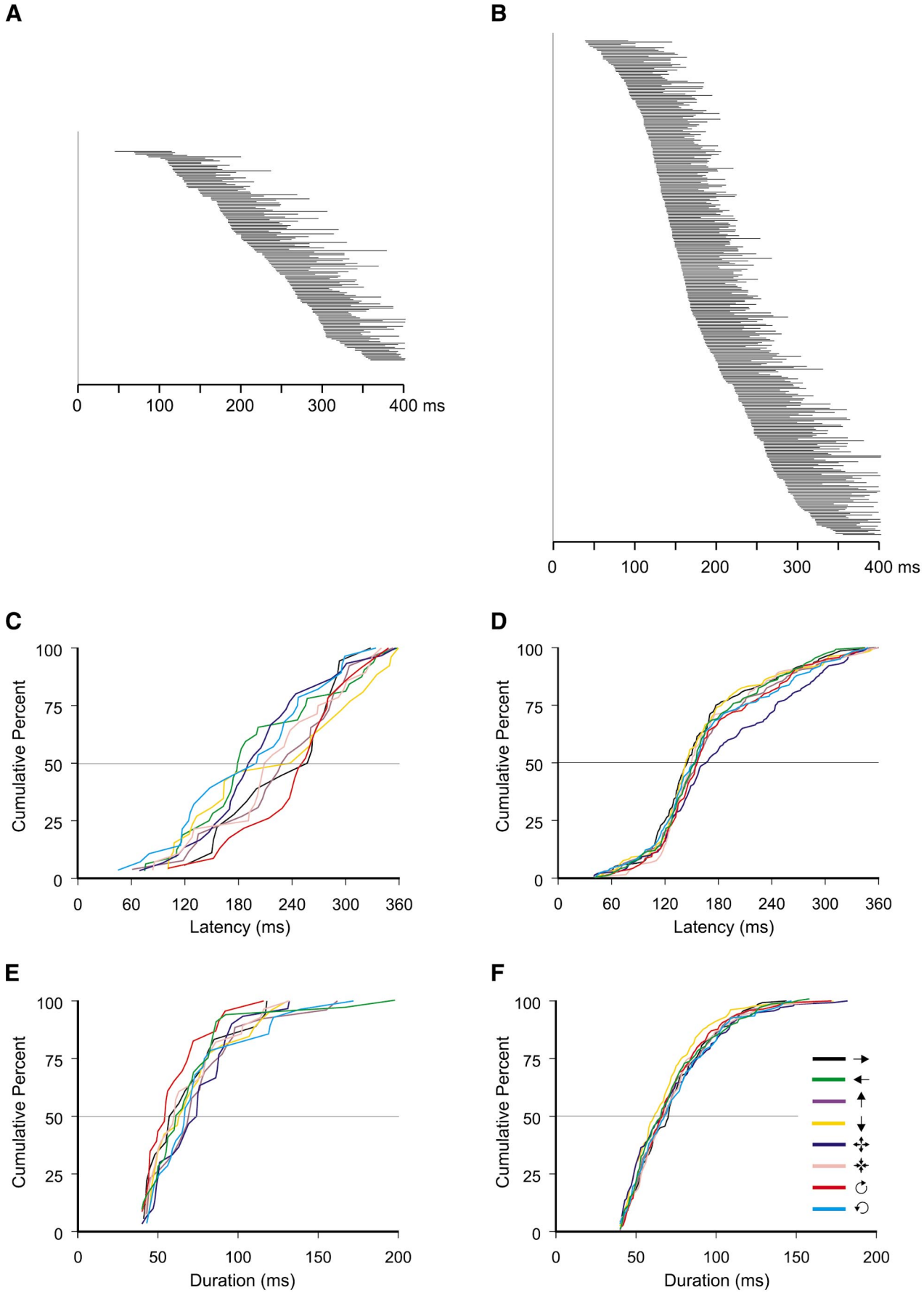

Downloaded from www.physiology.org/journal/jn at Univ of Minnesota (134.084.001.059) on April 13, 2019.

$$f(x, y) = b + k \exp\left\{ -\frac{1}{2(1-r^2)} \left[\left(\frac{x - x_0}{s_x} \right)^2 + \left(\frac{y - y_0}{s_y} \right)^2 - 2r \left(\frac{x - x_0}{s_x} \right) \left(\frac{y - y_0}{s_y} \right) \right] \right\}$$

where b and k define the offset and depth of the tuning, respectively; x_0 and y_0 specify the preferred position in the (x, y) plane; s_x and s_y characterize the width of the tuning along the two orthogonal axes; and r together with s_x and s_y define the angle of rotation in the (x, y) plane as follows

$$\tan 2\theta = \frac{2rs_x s_y}{s_x^2 - s_y^2}$$

The polynomial function used was

$$f(x, y) = b_0 + b_1 x + b_2 y + b_3 x^2 + b_4 y^2 + b_5 xy$$

where b_0 is the offset and the combination of the coefficients b_1 to b_5 can define an ellipsoid, a paraboloid, or a hyperboloid. The least-squares method was used for curve fitting, using the function DRNLIN of the IMSL library (Digital Visual Fortran, Professional Edition 1998). The R^2 calculated and a detailed analysis of the residuals was performed (Draper and Smith 1981). Furthermore, the significant level of the R^2 was assessed using bootstrap ($n = 10{,}000$ bootstrap samples). The significant R^2 at $P < 0.05$ was ~0.46 for the double Gaussian and ~0.42 for the polynomial regression.

RESULTS

Neural responses to optic flow stimuli (Fig. 2)

The total number of cells with a statistically significant effect of visual stimulation in the ANOVA was three times greater in area 7a (370/587, 63%) than in motor cortex (148/693, 21.4%). The number of significant neurons to stimulus Motion condition, stimulus Location, and/or stimulus Motion condition × Location interaction are listed in Table 1. The proportion of cells with significant effects of different factors was not the same in both cortical areas, with a higher effect of Stimulus Location in area 7a and a larger effect of Motion condition in motor cortex. Overall, 79/148 (53.4%) motor cortical neurons and 102/370 (27.6%) neurons in area 7a showed a statistically significant effect of Motion condition; and 48/148 (32.4%) motor cortical neurons and 311/370 (84%) neurons in area 7a that showed a statistically significant effect of stimulus Location.

The results above were obtained by performing statistical analyses on square-rooted discharge rates. Although this is an appropriate transformation (see METHODS), we also analyzed the data without any transformation and obtained very similar results.

Onset latencies

Figure 3, *A* and *B*, shows the distribution of the response onset and duration for cells that showed a significant effect in the Poisson train analysis. The onset latency of response was significantly longer in the motor cortex (221.9 ± 6.07 ms; mean ± SE, $n = 150$) than in area 7a (180.1 ± 3.86 ms, $n = 353$; *t*-test, $P < 0.0001$). On the other hand, the duration of the response did not differ significantly between the two areas (69.02 ± 1.95 ms for the motor cortex and 72.7 ± 1.02 ms in area 7a; *t*-test, $P = 0.074$).

A different question concerns possible differences in onset times among stimulus motion conditions. Figure 3, *C* and *D*, shows cumulative functions of onset times separately for each stimulus motion condition. It can be seen that in the motor cortex (Fig. 3*C*) there was an a appreciable spread of these functions; the rank order of the eight stimulus motion conditions at the level of the median was as follows (*rank 1* being the earliest): leftward, expansion, CCW, contraction, upward, downward, CW, and rightward motion (medians: 181, 194, 201, 213.5, 231.5, 249, 255, and 259.5 ms, respectively). By contrast, in area 7 (Fig. 3*D*) the cumulative functions were very close; the rank order of the eight stimulus motion conditions at the level of the median was as follows: downward, rightward, contraction, leftward, CCW, upward, CW, and expansion motion (medians: 144, 145.5, 151, 154, 154, 155, 157, and 167 ms, respectively).

The cumulative functions of the response duration for each stimulus motion condition were close in both areas, as can be seen in Fig. 3, *E* and *F*. In the motor cortex (Fig. 3*E*) the rank order of the eight stimulus motion conditions at the level of the median was as follows (*rank 1* being the earliest): CW, rightward, contraction, leftward, downward, CCW, upward, and expansion motion (medians: 55, 60, 60.5, 63, 64.5, 67, 70, and 74.5 ms, respectively). Furthermore, in area 7a (Fig. 3*F*) the cumulative functions were closer than in motor cortex. The rank order of the response duration of the eight stimulus motion conditions in this area was as follows: downward, leftward, expansion, upward, contraction, CW, CCW, and rightward (medians: 62, 66, 66, 67, 67, 67, 68, and 71 ms, respectively).

Finally, the potential association between onset latency and response magnitude was assessed by performing a correlation analysis (Fig. 4, *A* and *B*). There were weak but statistically significant correlations in the two areas studied but also of different sign. Specifically, for the motor cortex, $r = 0.158$ ($P = 0.022$, $n = 211$), and for area 7, $r = -0.077$ ($P = 0.011$, $n = 1{,}100$).

Relative effect of type of stimulus motion

A different question concerns the relative strength of the responses with respect to the various kinds of stimulus motion. Two analyses were performed for this problem, for cells with a statistically significant Motion condition effect, as follows. In one analysis, the mean firing rates for the eight stimulus motion conditions were ranked, and the times for which a given stimulus condition was ranked first counted across cells. In the second analysis, Tukey tests (Zar 1996) were performed and the times counted for which the firing rate for a given stimulus condition was significantly larger than every other (taken pairwise). Overall, the ranking and Tukey test showed that the responses to expanding optic flow were the strongest, particu-

FIG. 3. *A* and *B*: response onset latencies and duration for motor (A, $n = 150$) and area 7a (B, $n = 353$) cells with a significant activation effect in the Poisson train analysis. Each line represents a cell, and its beginning and end are the average times of onset and offset of the response. *C* and *D*: cumulative functions of onset times for the 8 stimulus motion conditions for motor (*C*) and area 7 (*D*) cells. *E* and *F*: cumulative functions of response durations for the 8 stimulus motion conditions for motor (*E*) and area 7 (*F*) cells.

Downloaded from www.physiology.org/journal/jn at Univ of Minnesota (134.084.001.059) on April 13, 2019.

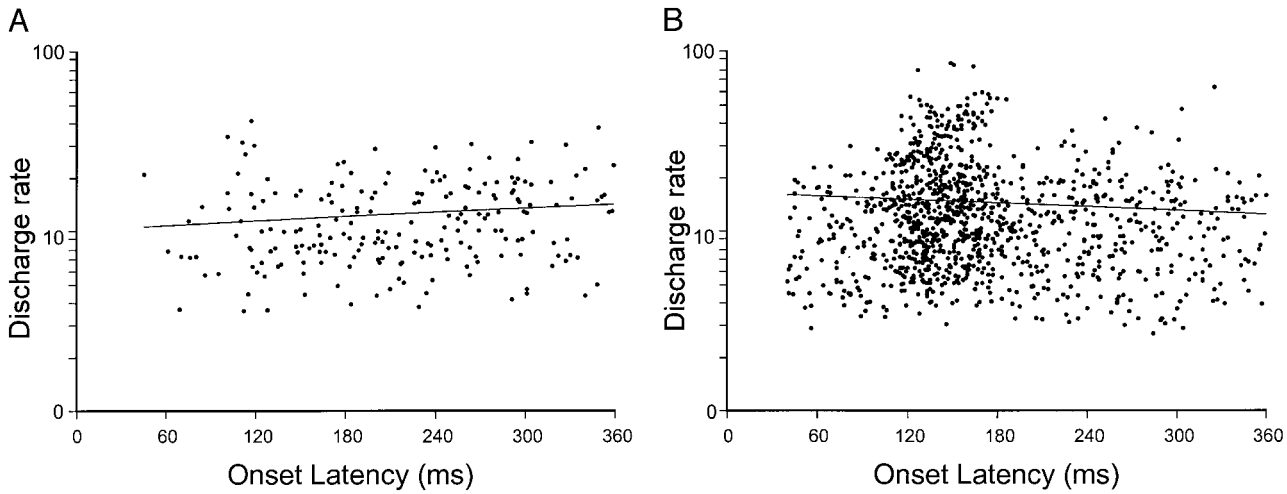

FIG. 4. *A* and *B*: scatter plots of the discharge rate observed during the cell response (i.e., the time from the onset to the offset of the response) against the onset time for motor cortex (*A*, $n = 221$) and area 7 (*B*, $n = 1{,}100$). Points represent cases with a significant activation effect in the Poisson train analysis. The discharge rates are plotted on a log-scale to normalize their distribution.

larly in the motor cortex. In addition, there was also a strong response to the rightward motion in area 7a, i.e., toward the contralateral side. The results of the ranking are shown in Fig. 5 for the motor cortex (Fig. 5*A*) and area 7a (Fig. 5*B*). These results were highly congruent with those obtained in the Tukey tests in both cortical areas (Spearman's rank correlation $\rho = 0.945$, $P = 0.0004$ for the motor cortex, and $\rho = 0.727$, $P = 0.027$ for area 7a). The corresponding total discharge frequency (i.e., number of cells × mean discharge rate per cell) is illustrated in Fig. 5*C* for the motor cortical population and in Fig. 5*D* for the population of area 7a cells.

Selectivity of cell response

We used the Poisson train analysis (Hanes et al. 1995) (see METHODS) to assess the presence of a neural response to a particular Motion condition, and, consequently, determine the specificity of the cell activity to the Motion conditions used. The results showed that 152/693 (21.9%) of the neurons in the

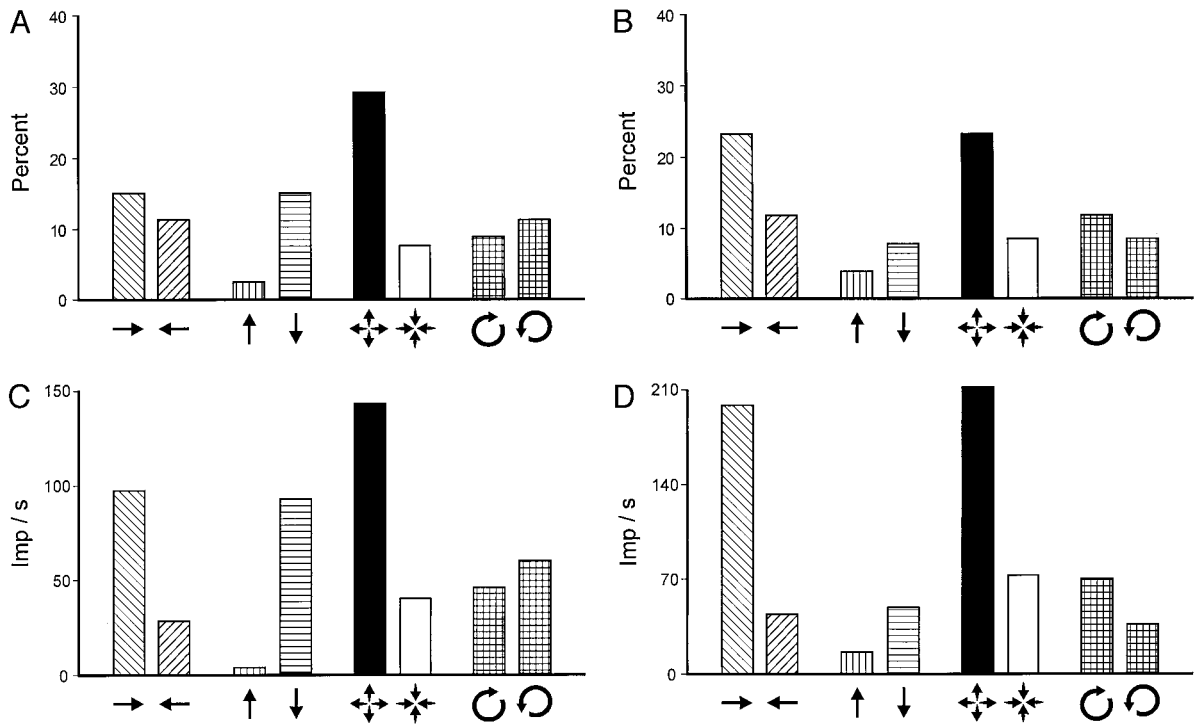

FIG. 5. *A*: percentages of times that a response to the optic flow stimuli shown underneath a bar was the highest among the 8 kinds of stimuli tested in the motor cortex ($n = 79$ cells that showed a statistically significant effect of stimulus Motion condition in the ANOVA). *B*: percentages of times that a response to the optic flow stimulus shown underneath a bar was the highest among the 8 kinds of stimuli tested in area 7a ($n = 102$ cells that showed a statistically significant effect as in *A*). *C*: average population activity for stimulus conditions noted when they were ranked 1st in the motor cortex. *D*: average population activity for the stimulus conditions noted when they were ranked 1st in area 7a.

Downloaded from www.physiology.org/journal/jn at Univ of Minnesota (134.084.001.059) on April 13, 2019.

motor cortex and 353/587 (60.1%) of the neurons in area 7a showed statistically significant responses for at least one Motion condition. As can be observed in Fig. 6, the majority of cells in motor cortex, 112/152 (73.7%), showed activation in only one stimulus condition, whereas 133/353 (37.7%) of the neurons in area 7a showed the same type of selectivity. In addition, 124/353 (35.1%) of neurons in area 7a responded to more than 3 stimulus Motion conditions, including 22 neurons that responded to all Motion conditions. No such neurons were observed in the motor cortex. Overall, the distribution of neurons with significant responses to one or more stimulus Motion condition (see Fig. 6) were differed significantly between the two cortical areas ($\chi^2 = 79$, DF $= 7$, $P < 10^{-10}$). Furthermore, the response to expansion was the most prevalent within the motor cortical cells that showed significant responses to only one stimulus Motion condition, but not clear prevalence was observed in the same type of neurons in area 7a (Table 2, $\chi^2 = 17.6$, DF $= 7$, $P = 0.014$).

As mentioned above, the monkeys were required to fixate their eyes on a central spot during stimulus presentation. The interpretation of the results above obviously depends on that condition being fulfilled. Indeed, the eyes remained fixated as required. This is illustrated in Fig. 7, which shows the relative frequency distribution of the *X-Y* eye position for all stimulus presentations. Adherence to fixation was also corroborated by the results of an analysis of eye velocity: we found that >99.2% of the tangential eye velocity values recorded during visual stimulus presentation were <150 DVA/s, a threshold commonly used to detect the occurrence of a saccade (Siegel and Read 1997). This percentage was >93.2% using a lower threshold of <50 DVA/s (Read and Siegel 1997).

Visual RFs in motor cortex

In general, there was not an obviously discernible visual RF structure in the neuronal responses of motor cortex (Fig. 8). However, for a detailed analysis, we used two different kinds of nonlinear regression (a double Gaussian and a polynomial) on the mean firing rate observed at the 25 stimulus locations. This analysis was performed on each of the eight Motion conditions for 75 neurons that showed significant effect in Stimulus Location and/or Motion condition × Location interaction in the ANOVA (total cases 600, see Table 1). For the double Gaussian regression, the median percent of variance accounted for (coefficient of determination, R^2) was 19%; the 25th and 75th percentiles were 1% (lack of convergence) and 32%, respectively. For the polynomial regression, the median R^2 was 21%; the 25th and 75th percentiles were 12 and 27%, respectively. In addition, only 6.3% (38/600) of the cases in the double Gaussian and 5.2% (31/600) in the polynomial fitting were significant in the bootstrap ($P < 0.05$). These results indicate that, although there can be some orderly variation in the spatial profile of cell response in few neurons, for most cells this was not the case. Therefore the modulation of motor cortical cell activity by optic flow stimuli described above does not reflect a RF structure.

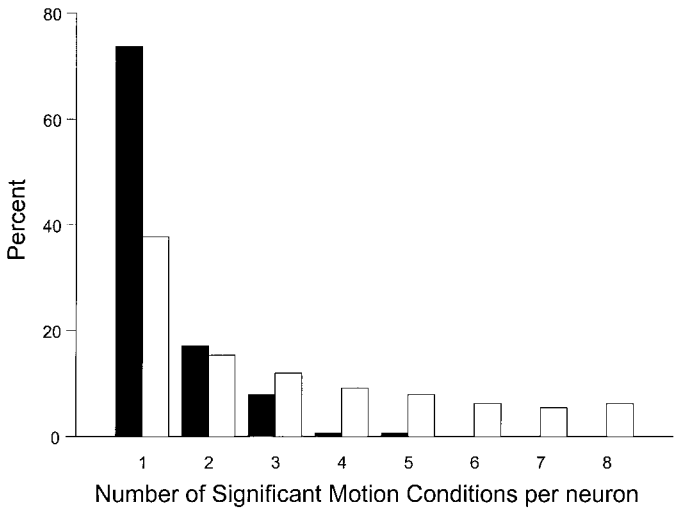

FIG. 6. Percentages of times that a cell showed significant responses in the Poisson train analysis to different numbers of stimulus Motion conditions in the motor cortex (■, $n = 152$) and area 7a (□, $n = 353$).

TABLE 2. *Numbers and percentages of neurons that showed a consistent response to only one stimulus motion condition in the Poisson spike train test*

Motion Condition	Motor Cortex	Area 7a
Right	4 (3.6)	21 (15.8)
Left	12 (10.7)	19 (14.3)
Up	16 (14.3)	17 (12.8)
Down	13 (11.6)	10 (7.5)
Expansion	20 (17.9)	21 (15.8)
Contraction	17 (15.1)	19 (14.3)
CW	14 (12.5)	20 (15)
CCW	16 (14.3)	6 (4.5)
Total	112 (100)	133 (100)

Numbers in parentheses are percentages. CW, clockwise; CCW, counterclockwise.

Visual RF structure in the area 7a

In contrast to the motor cortex, cells in area 7a typically showed clear cut RFs (see Figs. 9–11). The double Gaussian and polynomial regressions were performed in a total of 2,648 cases (8 Motion conditions × 331 neurons with significant effects in Stimulus Location and/or Motion condition × Location interaction in the ANOVA; see Table 1). For the double Gaussian regression, the median R^2 was 28%, and the 25th and 75th percentiles were 7 and 44%, respectively. For the polynomial regression, the median R^2 was 30%, and the 25th and 75th percentiles were 18 and 40%, respectively. In addition, 21.6% (572/2648) of the cases in the double Gaussian and 22.5% (597/2648) in the polynomial regression were significant in the bootstrap ($P < 0.05$). Therefore the RF structure observed with the visual inspection of the rasters was well explained by the two types of nonlinear regressions. However, we used the results of the double Gaussian regression for further analysis, since the parameters of this regression can be used directly to compare the visual RFs across neurons and conditions, and there was not a clear difference in the R^2 obtained with both regressions.

The regression models above were also evaluated by plotting the residuals against the predicted value (Draper and Smith 1981) that showed that they were distributed approximately evenly above and below zero without any particular pattern. This indicates that the models were adequate, that is that no additional terms were needed. This is not surprising since these models were essentially constructed for curve-fitting and therefore contained enough free parameters. Then the appropriate-

Downloaded from www.physiology.org/journal/jn at Univ of Minnesota (134.084.001.059) on April 13, 2019.

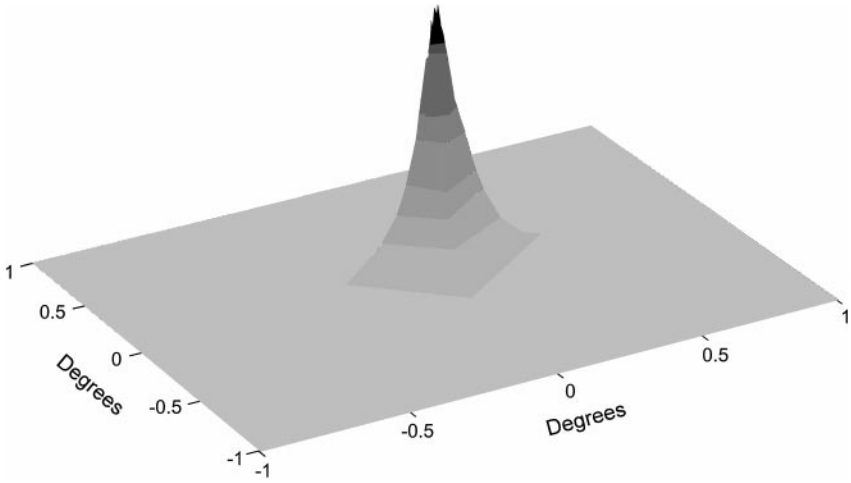

FIG. 7. Relative frequency distribution (in percent) of *x-y* eye position during stimulus presentation [N = 8,688,000 eye position samples: 181 cells (79 motor cortical cells + 102 area 7a cells) × 25 patch locations × 8 stimulus motion conditions × 3 repetitions × 80 samples/patch stimulation].

ness of the model implies that the R^2 can, in this case, serve as a proper assessment of the goodness-of-fit of the model.

Visual RF size in the area 7a

The half-height areas of the RFs, defined as the 50% of the maximum response in the significant Gaussian regressions with a positive depth of the tuning, k (excitatory responses, see METHODS), presented a wide range of values. We included only those neurons with a RF center inside the stimulation area for a total of 351 cases. The median of the half-height areas was 1022.1 DVA^2 and the 25th and 75th percentiles were 239.2 and 1,360.6 DVA^2, respectively. These areas did not change as a function of the RF center eccentricity (Fig. 12*A*). However, as is shown in Fig. 12*B*, the distribution of the center of the RFs in the horizontal axis (y_0) was slightly skewed to the right (contralateral to the recording sites). Bilateral RFs were common.

Density plots of neurons with positive (351 cases, 160 neurons; Fig. 13*A*) and negative (67 cases, 52 neurons; Fig. 13*B*) k values were obtained pulling together the half-height areas of significant RF. It is clear from Fig. 13*A* that the more dense portion of the visual field represented in area 7a is around 10 DVA, corresponding to the region of central vision, and that even if there is a small bias toward the right side there is a bilateral representation of the visual field. In addition, neurons with negative k spare the central location, where the FP is presented, at least in some Motion conditions.

Position invariance of optic flow selective responses in area 7a

Cells in area 7a with significant RF structure in the double Gaussian regression were also classified with respect to their selectivity to stimulus motion. The results of this classification showed that 106/244 (43.4%) of neurons had significant RFs to only one stimulus Motion condition, and that the number of neurons with significant RFs in different stimulus Motion Conditions decreased as the number of stimulus Motion Conditions increased. Examples of cells with a significant RFs in only one stimulus Motion condition (Fig. 9), to two stimulus Motion conditions (Fig. 10), and to all stimulus Motion condition (Fig. 11) are illustrated.

We performed an ANOVA on the cells with consistent responses during radial or circular motion (as assessed by the Poisson train analysis) and with significant RFs in the double Gaussian regression, to determine the presence of position invariance of the response across their RF. In this ANOVA we used the stimulus Location inside the RF as a factor and the discharge rate as the dependent variable. We found that 62.1% (82/132) of the cases did not show a significant effect of stimulus Location inside the RF, 12.1% (16/132) showed significant responses, and 25.8% (34/132) showed small RFs corresponding to only one location, and therefore the ANOVA could not be performed. These findings suggest that, in a large proportion of area 7a neurons, the responses during circular or radial motion stimulation do not depend on a linear summation of translation stimuli (Lagae et al. 1994), since these cells showed responses that were position invariant across the RF.

Finally, some cells in area 7a showed significant RFs in the rightward and leftward Motion conditions and showed an opponent vector organization (Motter and Mountcastle 1981; Steinmetz et al. 1987). We defined as inward opponent vector cells to those neurons with significantly larger responses in the left stimulated portion of the rightward direction and significantly larger responses in the right stimulated portion of the leftward direction (ANOVA). Conversely, outward opponent vector cells showed significantly larger responses in the right of the rightward direction and larger responses in the left of the leftward direction. The results indicated that 10 neurons showed inward (Fig. 10, *A* and *B*) and 4 neurons outward (Fig. 10*C*) opponent vector responses. In contrast, no neurons with responses during upward and downward Motion stimulation showed this type of opponent vector response organization.

Comparison of visual and motor effects on motor cortical neuronal activity

A different question concerns the magnitude of cell response during stimulus presentation, as compared with the changes in cell activity during force production by the contralateral hand. This was evaluated using a center → out, force exertion task. Of 514 motor cortical cells studied in both the motor and visual tasks, 388 (75.5%) showed a significant relation to either or both tasks, as follows: 284/388 (73.2%) cells showed a significant relation only to the motor task, 27/388 (7%) cells showed a significant relation only to the visual task, whereas the remaining 77/388 (19.8%) cells showed significant relations to both tasks. Therefore a total of 361/514 (70.2%) cells were

Downloaded from www.physiology.org/journal/jn at Univ of Minnesota (134.084.001.059) on April 13, 2019.

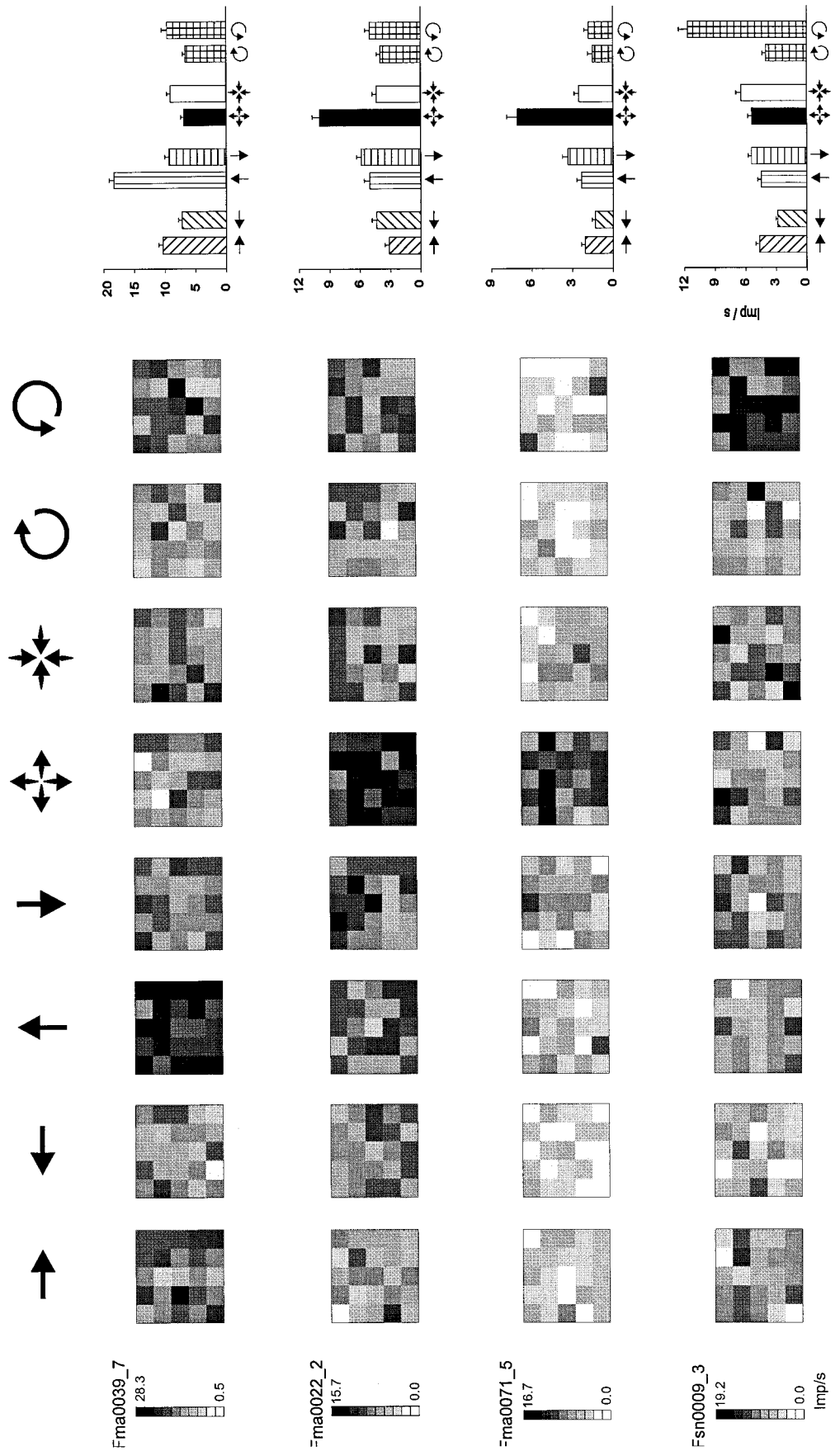

FIG. 8. Responses to optic flow stimuli of 4 motor cortical cells shown in a gray scale. These neurons showed clear responses to only 1 stimulus Motion condition. Bars indicate mean ± SE of response for each stimulus motion condition ($N = 75$ patch stimulations: 25 patches × 3 repetitions). For all these cells, only the stimulus Motion condition had a significant effect in the ANOVA (F-test; $P < 0.05$).

Downloaded from www.physiology.org/journal/jn at Univ of Minnesota (134.084.001.059) on April 13, 2019.

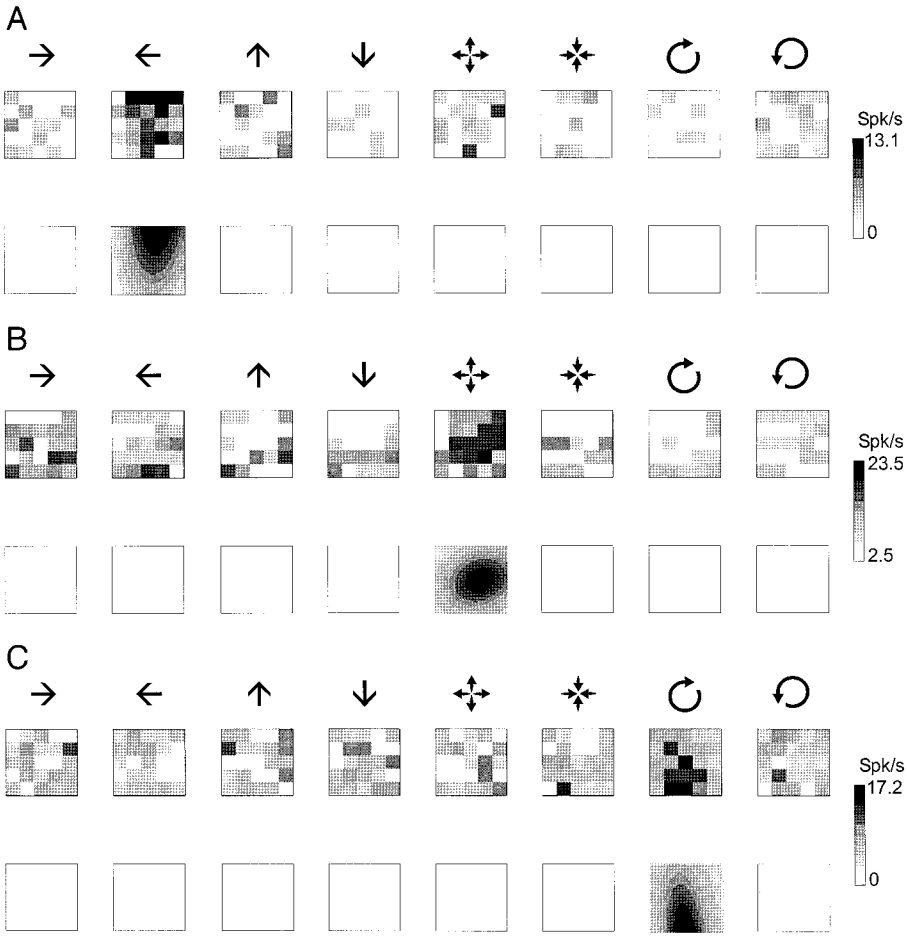

FIG. 9. Responses to optic flow stimuli of 3 cells in area 7a shown in a gray scale. For each neuron, the responses to the 25 stimulus Locations (*top*) and the corresponding double Gaussian fit (*bottom*, bootstrap $P < 0.05$) are shown. Motion conditions with nonsignificant double Gaussian regression are not shown. *A*: cell that showed a selective response to leftward stimulus motion. *B*: cell that showed a selective response to expanding optic flow. *C*: cell that showed a selective response to stimulus clockwise rotation.

related to the motor task, 104/514 (20.2%) were related to the visual task, and 49/514 (9.6%) did not show a significant relation to either task. These results are illustrated in Fig. 14 in the form of Venn diagrams.

The magnitude of motor cortical cell response was evaluated for the 77 cells that showed significant changes in activity in both tasks, as described in METHODS. We found that these changes (mean ± SE) were comparable, although significantly higher in the motor (19.1 ± 1.9 imp/s) than in the visual task (14.1 ± 1.0 imp/s; $P = 0.0015$, paired *t*-test); both of these values were significantly higher that the average activity (5.9 ± 0.7) during the control period of the motor task ($P < 10^{-10}$ for both tasks). For comparison, the average discharge rate of area 7a cells during the visual task (17.3 ± 2.4 imp/s, $n = 102$ stimulus Motion condition cells in the ANOVA above) was similar to the responses of motor cortical cells observed in the visual task ($P = 0.107$, independent samples *t*-test), but slightly smaller than the responses of the same cells tested in the motor task ($P = 0.004$, independent samples *t*-test). These results are illustrated in Fig. 15.

Finally, we analyzed more specifically the neuronal responses with respect to the directional domain (see METHODS). In the center → out task, 213/514 (41.4%) showed a significant directional effect in the ANOVA, and of those 190/213 (89.2%) were directionally tuned. In the visual task, stimulus location analysis, only 27/514 (5.2%) showed a significant effect of stimulus direction in the ANOVA, and of those only 1/27 (3.7%) was directionally tuned (see METHODS); in the visual task, motion condition analysis (using the 4 cardinal stimulus motions), 49/514 (9.5%) showed a significant stimulus motion effect in the ANOVA, and none were tuned.

EMG activity

There were practically no significant effects of stimulus motion presentation on muscular activity. The ANOVA and Tukey tests performed on the EMG activity of 13 shoulder, upper arm, and forearm muscles showed that only one muscle (anterior deltoid) in one monkey showed a significant Motion condition effect with a preference for rightward motion; however, the same muscle did not show any effect in the other monkey. This lack of a significant EMG change, as compared with the significant cell responses, could be due to a possible high variability in the EMG signal. However, this was not the case, for the geometric mean of the coefficient of variation for the EMG of all the muscles studied in both monkeys (see METHODS) was a modest 11%. In contrast, all muscles showed statistically significant changes during the center → out task (ANOVA).

Recording sites

The present results came from cells recorded in the primary motor cortex and area 7a. Photographs of the recording sites are shown in Fig. 16. Although no histological reconstruction of the recording sites was possible, several lines of evidence indicate that the presumed area 7a cells were indeed from that area. Specifically, *1*) the entry points of the penetrations were on the exposed surface of area 7a, *2*) penetrations were close to

Downloaded from www.physiology.org/journal/jn at Univ of Minnesota (134.084.001.059) on April 13, 2019.

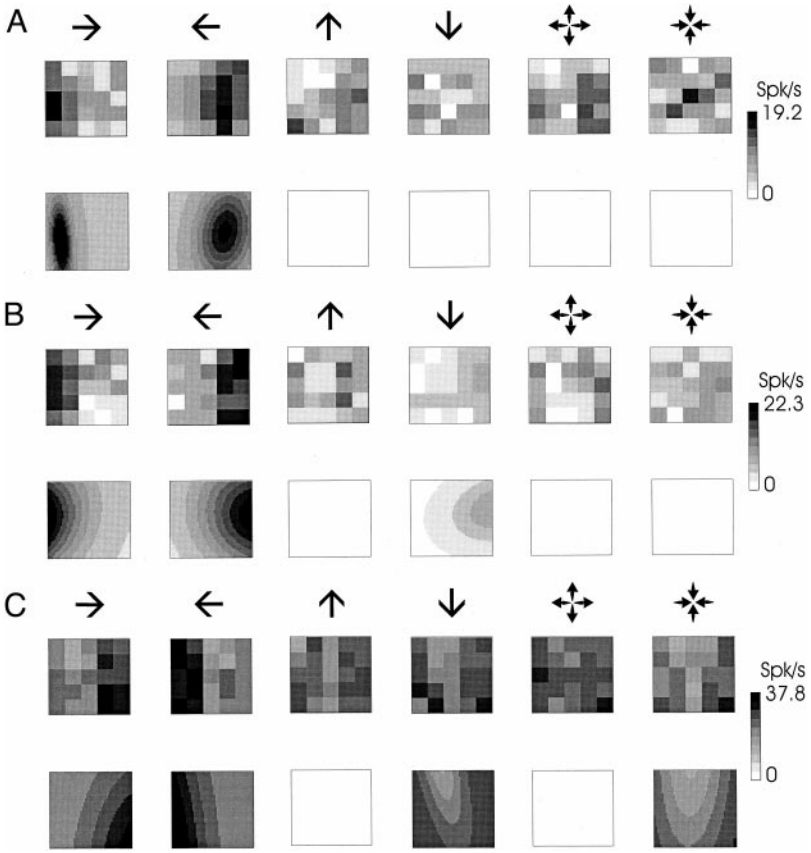

FIG. 10. Neurons with opponent response organization in area 7a with responses shown in a gray scale as in Fig. 9. *A*: neuron showing an inward opponent vector organization, with responses in the left part of the visual field during rightward motion and responses in the right part of the visual field in the left ward motion. *B*: another neuron with an inward opponent vector organization, with similar properties than in *A*. *C*: neuron showing an outward opponent vector organization, with responses in the right part of the visual field during rightward motion and responses in the left part of the visual field in the leftward motion.

being perpendicular to the cortical surface, and *3*) the depth of recordings were usually within 2 mm from the top of neural activity (median = 1,290 μm), both for those cells recorded from more centrally located penetrations and from those recorded from more anterior or posterior penetrations. In addition, the functional properties of cells recorded from more anterior or posterior penetrations were very similar to the rest of the group. Even when data from such anterior or posterior penetrations were removed from the sample, the remaining data were again very similar to those of the whole sample.

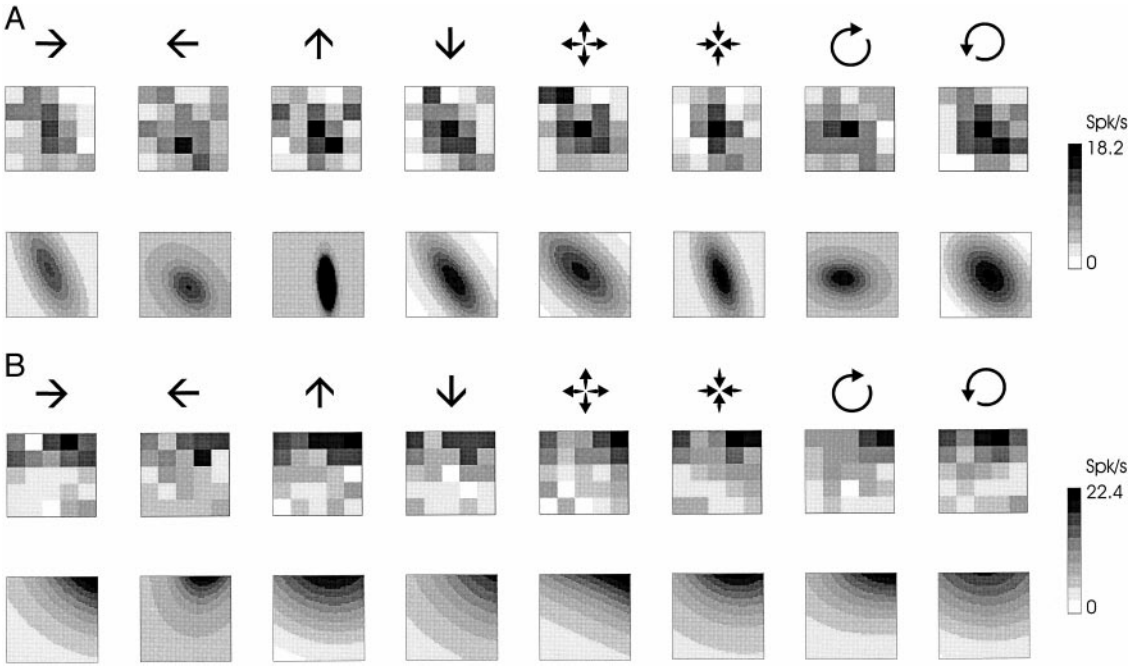

FIG. 11. Similar responses in all the different optic flow stimuli used in 2 cells of area 7a, shown in a gray scale as in Fig. 9. *A*: neuron with similar responses to optic flow stimuli in the center on the visual field. *B*: neuron showing similar responses to optic flow stimuli in the upper part of the visual field.

Downloaded from www.physiology.org/journal/jn at Univ of Minnesota (134.084.001.059) on April 13, 2019.

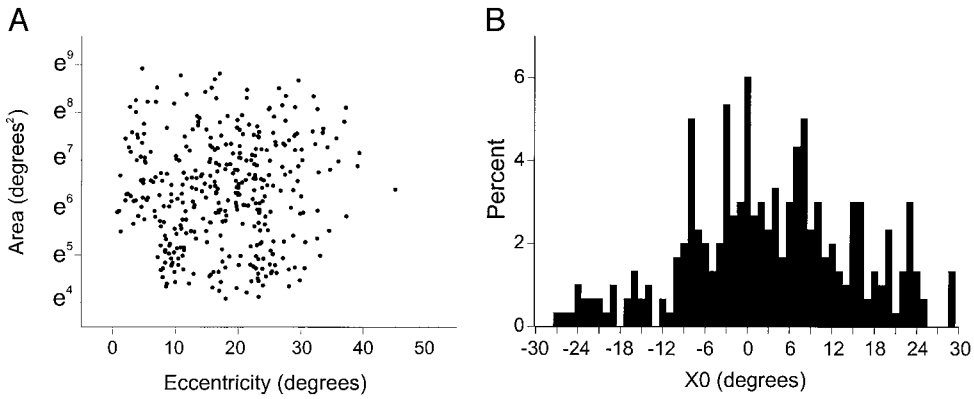

FIG. 12. *A*: relations between the receptive field (RF) size (half-height area) and the eccentricity of RF center for neurons with significant double Gaussian regression and excitatory peaks. Neurons with RF center outside the stimulation area were excluded, ending with 361 total cases from 160 neurons. Area 7a neurons did not show a relationship between RF area and eccentricity. *B*: histogram of the percentage of times that the horizontal component of the RF center (x_0) appeared at a particular position in the visual field on the same group of neurons shown in *A*. A clear bias to the right is observed.

DISCUSSION

Methodological considerations

Optic flow corresponds to the changes in the optic array induced by the relative motion between the subject and the environment. Information about optic flow is indispensable for encoding direction of heading, orientation, and visual navigation in three dimensional space, controlling posture and locomotion, and for the perception of moving objects and the selection of motor actions that allow the appropriate interaction with them (Koenderink 1986; Lee 1976, 1980). The objective of the present study was to investigate the neuronal responses

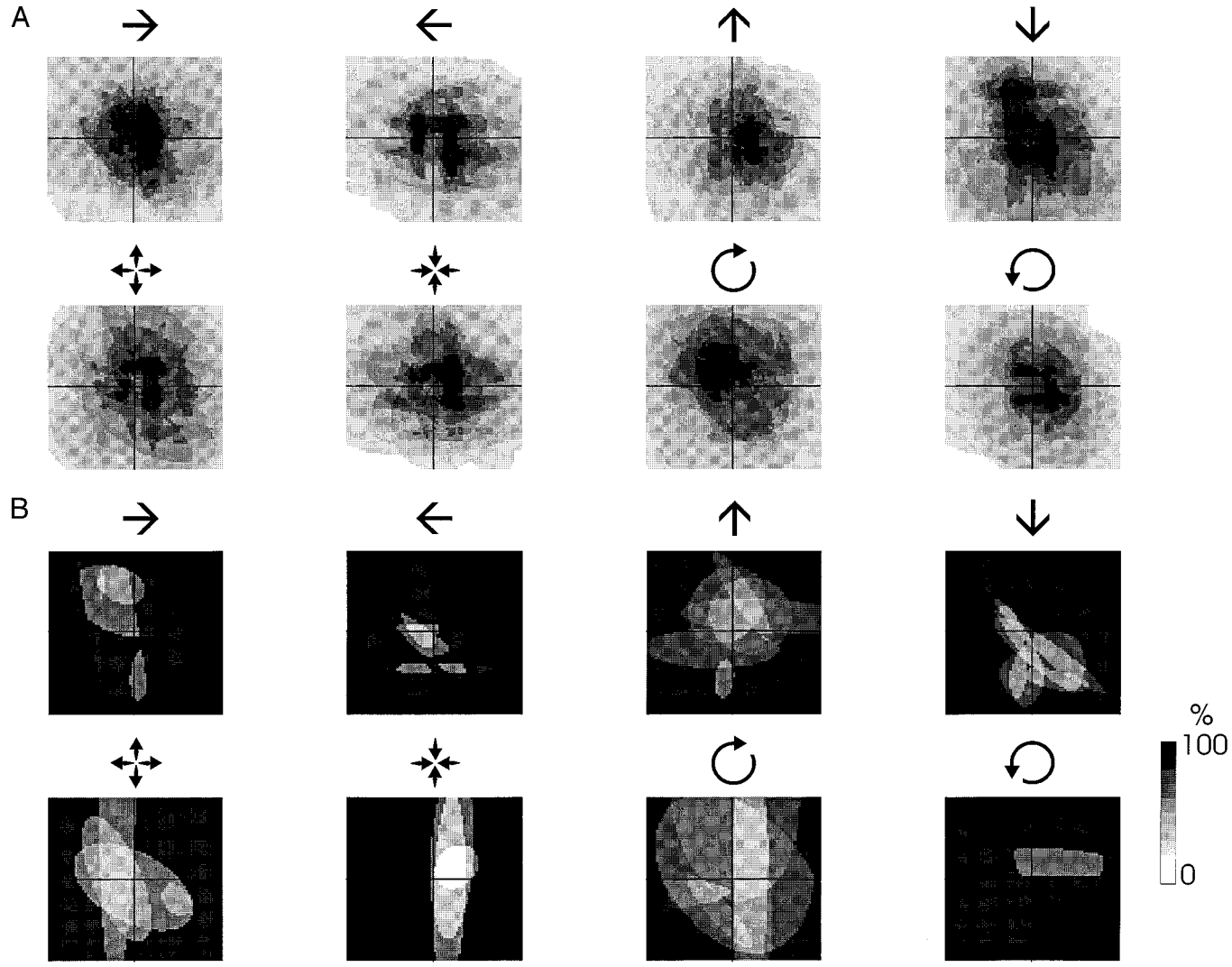

FIG. 13. Density plots obtained by combining the half-height areas of significant RF, shown in a gray scale. *A*: density plots per stimulus Motion condition of the RF with an excitatory peak (positive *k* in the double Gaussian regression, see METHODS). *B*: density plots per stimulus Motion condition of the RF with an inhibitory peak (negative *k* in the double Gaussian regression).

Downloaded from www.physiology.org/journal/jn at Univ of Minnesota (134.084.001.059) on April 13, 2019.

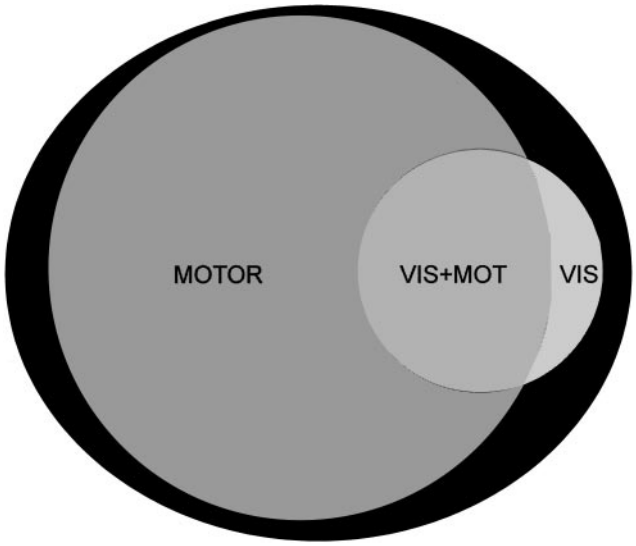

FIG. 14. Venn diagrams illustrating the 2 intersecting sets of motor-related ($n = 361$) and visual-related ($n = 104$) cells. The black ellipse denotes the total universe ($n = 516$ cells). The intersection contains 77 cells. The areas are proportional to the numbers above.

in area 7a and motor cortex to optic flow stimuli and to stimulus presentation at different parts of the visual field. Specifically, we wanted to assess these responses with respect to a good variety of stimulus motion characteristics and a detailed coverage of the visual field. These considerations led to the experimental design we used, namely the delivery of stimuli of 8 different kinds of motion to each one of 25 square patches covering a good area of the visual field. The stimuli consisted of random dots moving coherently to produce standard optic flow patterns, including translation, rotation, and radial motion. Since these stimuli were shown in patches of the visual field, one at a time, the resulting situation can be best described, in a natural setting, as an occluded optic flow stimulation, such as seen, for example, in a pilot of a plane during a flight: in this case, the full optic flow is occluded by the plane except for the patch of the cockpit window. Although this design provided the needed framework for our study, and has been used in previous studies (Lagae et al. 1994; Raiguel et al. 1997), it should be noted that it is different from other designs of studies aimed to investigate responses to optic flow or RF structure that have employed full field stimulation, static stimuli, or stimuli consisting of moving bars (see *Responses to optic flow in area 7a*). Our findings demonstrated the presence of clear responses of motor cortical cells to rectilinear, expanding, contracting, and rotatory (CW, CCW) optic flow stimuli that were presented passively, in the absence of a motor response. In addition, these results indicate that neurons in area 7a also respond to partial field optic flow stimuli, which qualitatively confirm findings of previous studies (Read and Siegel 1997; Siegel and Read 1997). These findings, and the comparison of the functional properties of both cortical areas during optic flow stimulation, will be discussed separately.

Motor cortical responses to optic flow

More than 20% of the motor cortical cells were modulated by optic flow stimuli. The proportion of the cells with significant stimulus Motion condition effects were approximately two times higher than those with stimulus Location effects. Interestingly, of all kinds of stimulus motion tested, responses to expanding optic flow were the strongest and the more prevalent.

The responses of motor cortical cells to optic flow stimuli, although of smaller magnitude, were comparable with those observed in the same cells during force exertion on a manipulandum. As expected, the large majority (361/514 = 70.2%) of cells were active in the latter task, and, of those, 77/361 (24.8%) responded to visual stimuli (Fig. 15). These findings establish visual motion information as a robust input to motor cortex.

Motor cortical responses to stimuli moving passively across the visual field, that is in the absence of anticipated response, were described previously (Port et al. 2001; Wannier et al. 1989). However, several important features distinguish the present study from those previous ones. First, optic flow stimuli were not used in either of those studies. Second, in the study by Wannier et al. (1989) visual stimulation consisted of moving the hand or a hand-held blinking light in front of monkeys that were not required to fixate their eyes; therefore the kind of stimulus motion delivered was not precisely controlled, and retinotopic information was not available. By contrast, in the present experiments both the kind of stimulus motion and the retinal location of the stimuli presented were precisely controlled. Finally, in both previous and the present study cell responses to moving visual stimuli were not associated with EMG activation.

With respect to the kinds of stimulus motion tested, all are typical elements of natural motions of objects in three-dimensional space. Therefore the motor cortical responses observed could reflect the availability to this structure of information concerning object motion that would apparently be very useful in planning a movement in relation to that object. Now, unlike other motions, expansion also provides information about the direction of heading. This literally "egocentric" case is unique because of the possibility of collision: action by the subject (i.e., approach or avoidance) would be in order. In that respect

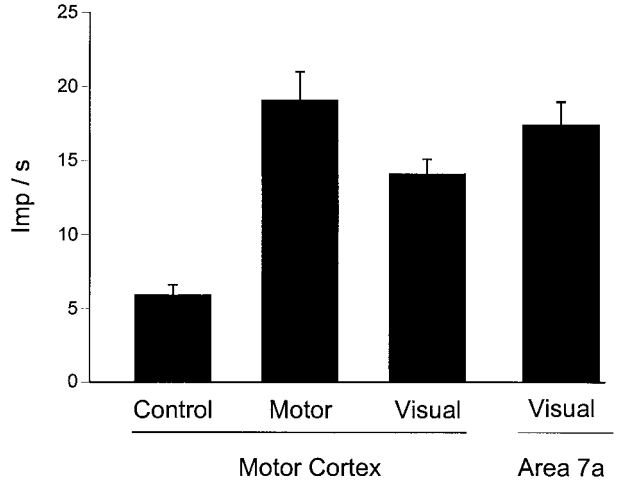

FIG. 15. Bars indicate the magnitude of cell activity in the motor cortex ($n = 77$) and area 7a ($n = 102$; mean ± SE) in the tasks indicated. Control, 500-ms-long period preceding force exertion in the center → out motor task; Motor, period from onset of peripheral stimulus until force threshold was exceeded in the center → out task; Visual, last 300-ms period of presentation of optic flow stimuli.

Downloaded from www.physiology.org/journal/jn at Univ of Minnesota (134.084.001.059) on April 13, 2019.

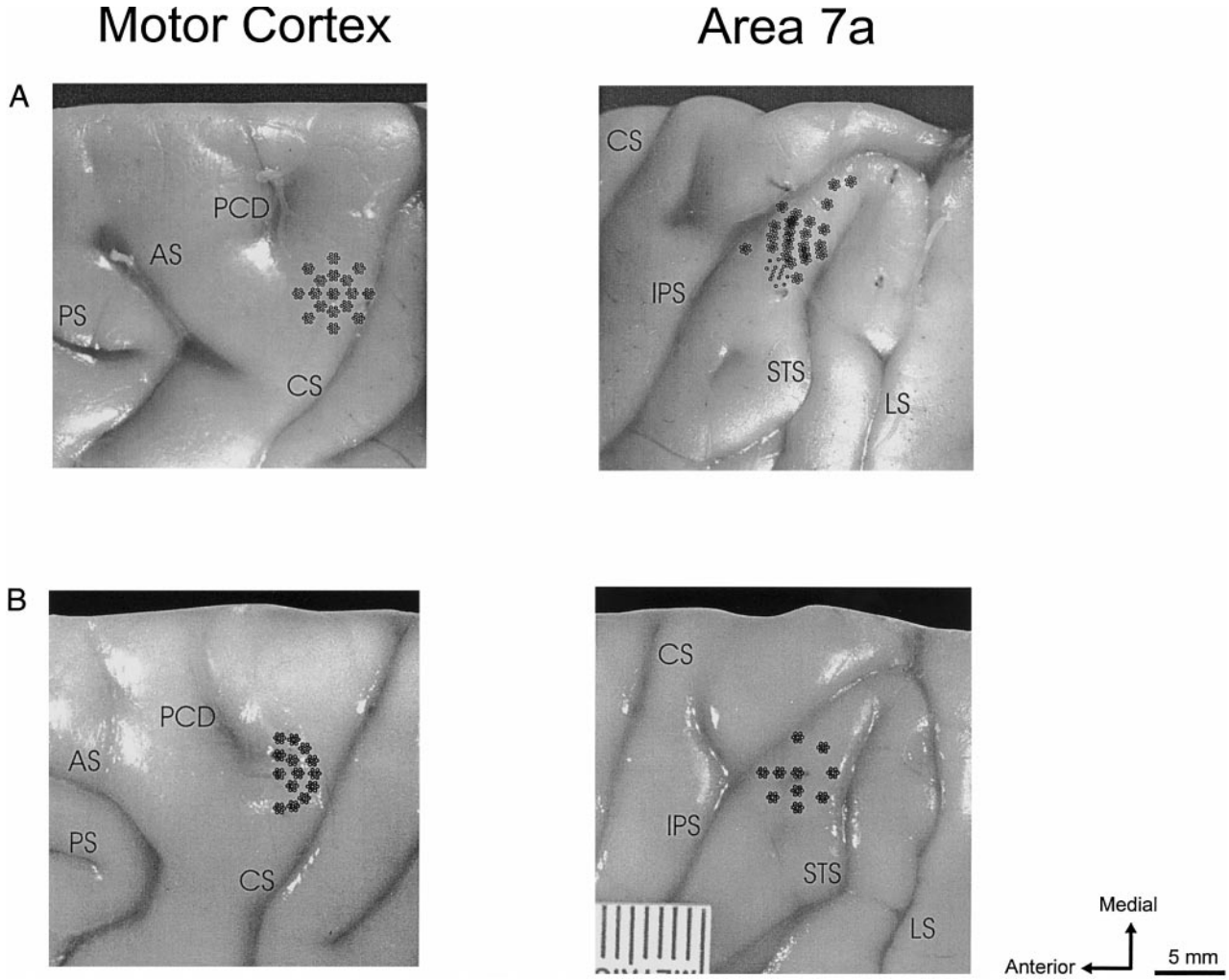

FIG. 16. Photographs of recording sites. Location on the brain surface of the sites of entry of the microelectrode penetrations (black dots; one per microelectrode) in the motor cortex and area 7a. *A*: *monkey 1*. *B*: *monkey 2*. CS, central sulcus; PS, principal sulcus; AS, arcuate sulcus; PCD, precentral dimple; IPS, intraparietal sulcus; STS, superior temporal sulcus; LS, lunate sulcus.

this situation differs qualitatively from that of rectilinear and/or rotatory stimulus motion in which case stimuli can be observed passively and action can be initiated by, but not forced on, the subject. In summary, then, if we assume an immobile observer, expanding optic flow would indicate, first of all, that a surface is approaching, and, second, would provide information on the direction of its approach. It is noteworthy that this kind of stimulus motion, conveying directional approach information, was effective in driving motor cortical cells and exerted, in fact, the strongest and most numerous effects. It is also remarkable that these effects were exerted in the absence of any required motor response. These findings suggest that directional approach information is available to the motor cortex for potential, but not obligatory, use in preparing a motor response. Of course, it is possible that the stimuli might have triggered neural events in the motor cortex in preparation of a motor response to interact with the stimulus in a certain part of the visual field even if not demanded by the experimenter. However, only few neurons that were directionally tuned in the center → out task were also tuned in the visual task, which suggests that the observed responses to optic flow stimuli were not related to the preparation of an intended motor response. Finally, the modulation of motor cortical cell activity by optic flow stimuli described above did not depend on a RF structure.

Responses to optic flow in area 7a

In the present study we found that ~60% of the neurons in area 7a were influenced by optic flow stimulation. Approximately three times more neurons were influenced by the location of the stimulus than by the kind of stimulus motion. In fact, a group of neurons in area 7a showed clear RF when stimulated with optic flow stimuli. The size, distribution, and modulation of the RF position by the type of stimulus Motion condition were characterized. In relation to the stimulus Motion condition effect, responses to expanding optic flow were the strongest.

Responses of area 7a cells to optic flow stimuli has been reported previously (Read and Siegel 1997; Siegel and Read 1997), and those findings were qualitatively replicated in the present study. For example, Siegel and Read (1997) found that ~40% of the cells in this area were sensitive to certain types of optic flow such as translation, expansion, contraction, rotation, and spiral motion. There were two major differences between the experimental design of those previous studies (Read and

Downloaded from www.physiology.org/journal/jn at Univ of Minnesota (134.084.001.059) on April 13, 2019.

Siegel 1997; Siegel and Read 1997) and this one. First, the speed of the stimuli differed, namely it ranged from ~8 to ~27 DVA/s (see Fig. 2 in Siegel and Read 1997), whereas it was fixed at 40 DVA/s in the present study; and second, in both of the former studies the monkeys performed a task that required a motor response to detect a change from a structured optic flow field motion to an unstructured motion, whereas in the present study the monkeys just maintained fixation. Although the results obtained in both studies are qualitatively similar, the substantial differences above do not permit a detailed quantitative comparison.

Several studies have determined the RF size and position of area 7a cells using static or moving visual stimuli (Andersen et al. 1990; Motter and Mountcastle 1981; Motter et al. 1987; Robinson et al. 1978). For example, Robinson et al. (1978) used a static 3×3 DVA spot of white light and found that the majority of area 7a cells possessed large, frequently bilateral RFs with a clear bias to the contralateral visual hemifield. The results of the present study confirmed these findings using optic flow stimuli, and, in addition, indicated that the RF size did not vary with stimulus eccentricity (Fig. 12, *A* and *B*), a phenomenon already observed in MST neurons (Raiguel et al. 1997). In addition, we found that most of the RFs in area 7a showed a excitatory peak. When all these RFs were superimposed, it was found that the foveal region (10 DVA diameter circle) was most densely mapped (Fig. 13*A*). However, other neurons showed an inhibitory peak in their RF, which could include the foveal region; this means that these neuons did not respond to stimulation of the foveal region, a phenomenon called foveal sparing and fully characterized by Mountcastle and collaborators (Motter and Mountcastle 1981; Motter et al. 1987).

An important feature of area 7a cells is their responsiveness to moving as compared with static visual stimuli. Most of these cells are sensitive to the direction of bars being translated across the visual field, and a subset of these cells respond selectively to stimuli moving toward the FP (inward opponent vector neurons) or away the FP (outward opponent vector neurons) (Motter and Mountcastle 1981; Motter et al. 1987). The opponent vector organization observed in area 7a was considered well suited to be involved in the analysis of optic flow during locomotion or in the manipulation of objects by the hands (Motter and Mountcastle 1981; Steinmetz et al. 1987). However, in a recent study in which the response of area 7a cells to translating bars and optic flow stimuli was compared, it was found that, in general, neurons with opponent vector organization did not respond to expanding or contracting optic flow stimuli (Siegel and Read 1997). Therefore these observations suggest that two types of high-order visual motion processing can occur in area 7a; namely *1*) the encoding of spatial information from motion during optic flow stimulation and *2*) the processing of objects moving inward or outward across the peripheral edges of the visual fields, i.e., toward or away from the center of gaze (opponent vector organization). In the present study we observed both types of high-order processing, namely cells that responded to small field radial optic flow stimuli (Fig. 9*B*), and cells in which the RF changed position in an opponent vector organization, particularly within the leftward and rightward motion conditions (Fig. 10, *A–C*). The inward or outward opponent vector cells did not respond to expanding or contracting optic flow stimuli, a finding that supports the idea that such responses are probably related to the processing of objects moving in relation to the subject.

The results of the analysis of the RF structure in area 7a in this and earlier studies (Motter and Mountcastle 1981; Motter et al. 1987; Mountcastle et al. 1975) suggest that the RF size and position are a function of the behavioral state of the subject and the stimulus parameters used. Indeed, we found that the location of the RF could be influenced by the kind of stimulus Motion condition; for example, the RF could be relocated, depending on the opponent vector organization of the response to left- and rightward stimuli (Fig. 10, *A–C*), whereas, in other cases, the RF was similar size and location in all stimulus Motion conditions (Fig. 11, *A* and *B*).

Comparison between motor cortex and area 7a

There were three times more neurons responding to optic flow stimuli in area 7a than in the motor cortex. This in fact is not surprising, since for over 30 yr area 7a have been considered an important associative node involved in visual motion processing and as part of the visual dorsal stream. Responses to optic flow stimuli have been described in several other brain areas including the middle temporal (MT) area (Lagae et al. 1994), the medial superior temporal (MST) area (Duffy and Wurtz 1991a,b; Graziano et al. 1994; Lagae et al. 1994, Orban et al. 1995; Saito et al. 1986; Tanaka and Saito 1989; Tanaka et al. 1986, 1989), the ventral intraparietal area (Schaafsma and Duysens 1996), and the anterior superior temporal polysensory area (Anderson and Siegel 1999). With respect to the extent of the visual field stimulated, both whole field and partial field stimulations have been used.

Information on onset times of neuronal changes in activity indicates that the motor cortical sensitivity to moving visual stimuli could be mediated by corticocortical circuits. Very short onset times to the presentation of such stimuli have been reported for areas MT (Lagae et al. 1994) and MST (Duffy and Wurtz 1997; Lagae et al. 1994), with median values of <100 ms, for speeds of motion comparable with that used in the present study (e.g., 40 DVA/s for rectilinear, expansion, and contraction stimuli). We observed longer onset times in area 7a with a mean of 180.1 ms. Thus the motor cortical mean onset time of 221.9 ms observed in the present study is ~40 ms longer than that in area 7a, and both motor and parietal onset times are longer than those observed in areas MT and MST above. Although the exact corticocortical pathways for transmission of stimulus motion information are not known, the ordering of the onset times above suggests a progression from temporal to parietal to frontal areas. However, there seems to be an increase in the specificity of neuronal responses to moving visual stimuli, from temporal to frontal areas: typically cells in MT (Lagae et al. 1994), MST (Duffy and Wurtz 1991a,b; Graziano et al. 1994; Lagae et al. 1994; Orban et al. 1995; Saito et al. 1986; Tanaka and Saito 1989; Tanaka et al. 1986, 1989), and area 7a respond to more than one kind of optic flow stimuli, whereas in motor cortex most cells responded to just one kind. For example, we found that only 37.79% of cells in area 7a responded consistently to only one kind of stimulus motion as compared with 73.7% in motor cortex. This indicates a segregation at the motor cortical level of subsets of cells that are selective for a particular type of motion, which, in turn, suggests that, e.g., objects moving in

Downloaded from www.physiology.org/journal/jn at Univ of Minnesota (134.084.001.059) on April 13, 2019.

different ways might engage nonoverlapping sets of motor cortical cells for possible action.

We thank D. N. Lee for advice on aspects of the visual stimuli used.

This work was supported by National Institute of Mental Health Grant PSMH-48185, the United States Department of Veterans Affairs, and the American Legion Brain Sciences Chair.

REFERENCES

ALEXANDER GE AND CRUTCHER MD. Neural representations of the target, goal of visually guided arm movements in three motor areas of the monkey. *J Neurophysiol* 64: 164–177, 1990a.

ALEXANDER GE AND CRUTCHER MD. Preparation for movement: neural representations of intended direction in three motor areas of the monkey. *J Neurophysiol* 64: 133–149, 1990b.

ANDERSEN RA. Multimodal integration for the representation of space in the posterior parietal cortex. *Philos Trans R Soc Lond B Biol Sci* 352: 1421–1428, 1997.

ANDERSEN RA, ASANUMA C, ESSICK G, AND SIEGEL RM. Corticocortical connections of anatomically and physiologically defined subdivisions within the inferior parietal lobule. *J Comp Neurol* 296: 65–113, 1990.

ANDERSON KC AND SIEGEL RM. Optic flow selectivity in the anterior superior temporal polysensory area STPa, of the behaving monkey. *J Neurosci* 19: 2681–2692, 1999.

BARLOW RJ. *Statistics—A Guide to the Use of Statistical Methods in the Physical Sciences.* Chichester, UK: Wiley, 1989.

COX DR AND LEWIS PAW. *The Statistical Analysis of Series of Events*. London: Chapman and Hall, 1966.

DRAPER NR AND SMITH H. *Applied Regression Analysis*. New York: Wiley, 1981.

DUFFY CJ AND WURTZ RH. Sensitivity of MST neurons to optic flow stimuli. I. A continuum of response selectivity to large-field stimuli. *J Neurophysiol* 65: 1329–1345, 1991a.

DUFFY CJ AND WURTZ RH. Sensitivity of MST neurons to optic flow stimuli. II. Mechanisms of response selectivity revealed by small-field stimuli. *J Neurophysiol* 65: 1346–1359, 1991b.

DUFFY CJ AND WURTZ RH. Multiple temporal components of optic flow responses in MST neurons. *Exp Brain Res* 114: 472–482, 1997.

EVARTS EV. *Handbook of Physiology. The Nervous System. Motor Control.* Bethesda, MD: Am. Physiol. Soc., 1981, sect. 1, vol. II, p. 1083–1120.

GEORGOPOULOS AP, ASHE J, SMYRNIS N, AND TAIRA M. Motor cortex and the coding of force. *Science* 256: 1692–1695, 1992.

GEORGOPOULOS AP, KALASKA JF, CAMINITI R, AND MASSEY JT. On the relations between the direction of two-dimensional arm movements and cell discharge in primate motor cortex. *J Neurosci* 2: 1527–1537, 1982.

GEORGOPOULOS AP, LURITO JT, PETRIDES M, SCHWARTZ AB, AND MASSEY JT. Mental rotation of the neuronal population vector. *Science* 243: 234–236, 1989.

GEORGOPOULOS AP, SCHWARTZ AB, AND KETTNER RE. Neuronal population coding of movement direction. *Science* 233: 1416–1419, 1986.

GRAZIANO MSA, ANDERSEN RA, AND SNOWDEN RJ. Tuning of MST neurons to spiral motions. *J Neurosci* 14: 54–67, 1994.

HANES DP, THOMPSON KG, AND SCHALL JD. Relationship of presaccadic activity in frontal eye field and supplementary eye field to saccade initiation in macaque: Poisson spike train analysis. *Exp Brain Res* 103: 85–96, 1995.

KOENDERINK JJ. Optic flow. *Vision Res* 26: 161–180, 1986.

LAGAE L, MAES H, RAIGUEL S, XIAO DK, AND ORBAN GA. Responses of macaque STS neurons to optic flow components: a comparison of areas MT and MST. *J Neurophysiol* 71: 1597–1626, 1994.

LEE D, PORT NL, KRUSE W, AND GEORGOPOULOS AP. *Neuronal Ensembles: Strategies for Recording and Decoding*. New York: Wiley, 1998, p. 117–136.

LEE DN. A theory of visual control of braking based on information about time-to-collision. *Perception* 5: 437–459, 1976.

LEE DN. The optic flow field: the foundation of vision. *Philos Trans R Soc Lond B Biol Sci* 290: 169–179, 1980.

LURITO JT, GEORGAKOPOULOS T, AND GEORGOPOULOS AP. Cognitive spatial-motor processes. 7. The making of movements at an angle from a stimulus direction: studies of motor cortical activity at the single cell and population levels. *Exp Brain Res* 87: 562–580, 1991.

MOTTER BC AND MOUNTCASTLE VB. The functional properties of the light-sensitive neurons of the posterior parietal cortex studied in waking monkeys: foveal sparing and opponent vector organization. *J Neurosci* 1: 3–26, 1981.

MOTTER BC, STEINMETZ MA, DUFFY CJ, AND MOUNTCASTLE VB. Functional properties of parietal visual neurons: mechanisms of directionality along a single axis. *J Neurosci* 7: 154–176, 1987.

MOUNTCASTLE VB, LYNCH JC, GEORGOPOULOS A, SAKATA H, AND ACUNA C. Posterior parietal association cortex of the monkey: command functions for operations within extrapersonal space. *J Neurophysiol* 38: 871–908, 1975.

MOUNTCASTLE VB, REITBOECK HJ, POGGIO GF, AND STEINMETZ MA. Adaptation of the Reitboeck method of multiple microelectrode recording to the neocortex of the waking monkey. *J Neurosci Methods* 36: 77–84, 1991.

ORBAN GA, DUPONT P, DE BRUYN B, VOGELS R, VANDENBERGHE R, AND MORTELMANS L. First order analysis of optical flow in the monkey brain. *Proc Natl Acad Sci USA* 89: 2295–2299, 1995.

PORT NL, KRUSE W, LEE D, AND GEORGOPOULOS AP. Motor cortical activity during interception of moving targets. *J Cogn Neurosci* 13: 306–318, 2001.

RAIGUEL S, VAN HULLE MM, XIAO DK, MARCAR VL, LAGAE L, AND ORBAN GA. Size and shape of receptive fields in the medial superior temporal area (MST) of the macaque. *Neuroreport* 8: 2803–2808, 1997.

READ HL AND SIEGEL RM. Modulation of responses to optic flow in area 7a by retinotopic and oculomotor cues in monkey. *Cereb Cortex* 7: 647–661, 1997.

ROBINSON DL, GOLDBERG ME, AND STANTON GB. Parietal association cortex in the primate: sensory mechanisms and behavioral modulations. *J Neurophysiol* 41: 910–932, 1978.

SAITO H, YUKIE M, TANAKA K, HIKOSAKA K, FUKADA Y, AND IWAI E. Integration of direction signals of image motion in the superior temporal sulcus of the macaque monkey. *J Neurosci* 6: 145–157, 1986.

SCHAAFSMA SJ AND DUYSENS J. Neurons in the ventral intraparietal area of awake macaque monkey closely resemble neurons in the dorsal part on the medial superior temporal area in their responses to optic flow patterns. *J Neurophysiol* 76: 4056–4068, 1996.

SCHWARTZ AB, KETTNER RE, AND GEORGOPOULOS AP. Primate motor cortex and free arm movements to visual targets in three-dimensional space. I. Relations between single cell discharge and direction of movement. *J Neurosci* 8: 2913–2927, 1988.

SIEGEL RM AND READ HL. Analysis of optic flow in the monkey parietal area 7a. *Cereb Cortex* 7: 327–346, 1997.

SNEDECOR GW AND COCHRAN WG. *Statistical Methods*. Ames, IA: The Iowa State Univ. Press, 1989.

STEINMETZ MA, MOTTER BC, DUFFY CJ, AND MOUNCASTLE VM. Functional properties of parietal visual neurons: radial organization of directionalities within the visual field. *J Neurosci* 7: 177–191, 1987.

TANAKA K, FUKADA Y, AND SAITO HA. Underlying mechanism of the response specificity of expansion/contraction and rotation cells in the dorsal part of the medial superior temporal area of the macaque monkey. *J Neurophysiol* 62: 642–656, 1989.

TANAKA K, HIKOSAKA K, SAITO H, YUKIE M, FUKADA Y, AND IWAI E. Analysis of local and wide-field movements in the superior temporal visual areas of the macaque monkey. *J Neurosci* 6: 134–144, 1986.

TANAKA K AND SAITO HA. Analysis of motion of the visual field by direction, expansion/contraction, and rotation cells clustered in the dorsal part of the medial superior temporal area of the macaque monkey. *J Neurophysiol* 62: 626–641, 1989.

TUKEY JW. *Exploratory Data Analysis.* Reading, MA: Addison Wesley, 1977.

WANNIER TM, MAIER MA, AND HEPP-REYMOND MC. Responses of motor cortex neurons to visual stimulation in the alert monkey. *Neurosci Lett* 98: 63–68, 1989.

ZAR JH. *Biostatistical Analysis*. Englewood Cliffs, NJ: Prentice Hall, 1996.

ZHANG J, RIEHLE A, REQUIN J, AND KORNBLUM S. Dynamics of single neuron activity in monkey primary motor cortex related to sensorimotor transformation. *J Neurosci* 17: 2227–2246, 1997.

Downloaded from www.physiology.org/journal/jn at Univ of Minnesota (134.084.001.059) on April 13, 2019.